5′ Modifications Improve Potency and Efficacy of DNA Donors for Precision Genome Editing

Krishna S Ghanta[1,9], Zexiang Chen[1,9], Aamir Mir[1,10], Gregoriy A Dokshin[1,10], Pranathi M Krishnamurthy[1], Yeonsoo Yoon[3], Judith Gallant[3,11], Ping Xu[3,11], Xiao-Ou Zhang[4], Ahmet Ozturk[1], Masahiro Shin[5], Feston Idrizi[5], Pengpeng Liu[5], Hassan Gneid[1,2], Nathan D Lawson[5,6,7], Jaime A Rivera-Pérez[3], Erik J Sontheimer[1,6,7*], Jonathan K Watts[1,2*] and Craig C Mello[1,7,8*]

Author Affiliations:

1. RNA Therapeutics Institute, University of Massachusetts Medical School, Worcester, MA 01605
2. Department of Biochemistry and Molecular Pharmacology, University of Massachusetts Medical School, Worcester, Massachusetts 01605
3. Department of Pediatrics, Division of Genes and Development, University of Massachusetts Medical School, Worcester, MA
4. Program in Bioinformatics and Integrative Biology, University of Massachusetts Medical School, Worcester, MA
5. Department of Molecular, Cell and Cancer Biology, University of Massachusetts Medical School, Worcester, Massachusetts, USA
6. Li Weibo Institute for Rare Diseases Research, University of Massachusetts Medical School, Worcester, MA, USA
7. Program in Molecular Medicine, University of Massachusetts Medical School, 368 Plantation Street, Worcester, MA, 01605 United States
8. Howard Hughes Medical Institute, University of Massachusetts Medical School, Worcester, MA, USA
9. These authors contributed equally
10. These authors contributed equally
11. These authors contributed equally

Present Address- A.M: Inscripta Therapeutics, Pleasanton, CA; G.A.D: Vertex Pharmaceuticals, Boston, MA; P.M.K: Bristol Myer Squibb, Cambridge MA.

* Correspondence to Erik.Sontheimer@umassmed.edu, Jonathan.Watts@umassmed.edu, Craig.Mello@umassmed.edu.

35 **Running Title:** Modified donors improve HDR efficacy.

36 **Key Words:** CRISPR, HDR, Modified donors, Chemical modifications

37 **Corresponding Authors:** Erik J. Sontheimer, Jonathan K. Watts and Craig C. Mello

38 **Mailing Address:**

39 RNA Therapeutics Institute,

40 University of Massachusetts Medical School,

41 368 Plantation Street, AS5-2049

42 Worcester, MA 01605, USA.

43 Phone: 508-845-1602

Abstract

Nuclease-directed genome editing is a powerful tool for investigating physiology and has great promise as a therapeutic approach to correct mutations that cause disease. In its most precise form, genome editing can use cellular homology-directed repair (HDR) pathways to insert information from an exogenously supplied DNA repair template (donor) directly into a targeted genomic location. Unfortunately, particularly for long insertions, toxicity and delivery considerations associated with repair template DNA can limit HDR efficacy. Here, we explore chemical modifications to both double-stranded and single-stranded DNA-repair templates. We describe 5′-terminal modifications, including in its simplest form the incorporation of triethylene glycol (TEG) moieties, that consistently increase the frequency of precision editing in the germlines of three animal models (*Caenorhabditis elegans*, zebrafish, mice) and in cultured human cells.

Introduction

Precision genome editing by HDR often requires cells to use exogenously supplied DNA templates (donors) to repair targeted double-strand breaks (DSBs). Maximizing precision genome editing, therefore, requires understanding both how cells respond to DSBs and to exogenous donors. These responses can be influenced by many variables, including cell-intrinsic factors (e.g., genetics, cell type, and cell cycle stage) and cell-extrinsic factors (e.g., donor length, strandedness, and chemistry) [1-11]. Each of these variables can influence the relative efficiency of HDR compared to competing DSB repair pathways, such as non-homologous end joining (NHEJ) [12-15].

In many organisms and cell types, high HDR efficiencies are readily achieved using short single-stranded oligodeoxynucleotide (ssODN) donor templates that permit single base changes or short insertions or deletions. However, HDR is frequently less efficient when longer double-stranded DNA (dsDNA) templates are used as donors. It is not known why longer DNA donors yield lower rates of HDR. In many cell types, high concentrations of dsDNA cause cytotoxicity, limiting the number of long donor molecules that can be safely delivered into cells. In addition,

71 due to their size, long donor molecules may not transit the nuclear envelope as efficiently, reducing
72 the effective concentration at the site of repair, or requiring cell division to gain access to the target
73 locus. Moreover, end-joining ligation reactions assemble linear dsDNA molecules into
74 concatemers in eukaryotic cells [16-20], further limiting the number of individual donor molecules
75 and their ability to diffuse to their DSB target sites.

76 In an effort to improve nuclear delivery and HDR efficacy, we incorporated 5′
77 modifications into the donor molecules, including a simple triethylene glycol (TEG) moiety, a 2′–
78 *O*–methyl (2′OMe) RNA::TEG modification, and a peptide nucleic acid (PNA) comprising the
79 SV40 nuclear localization signal (NLS) (see Methods). These 5′ modified donors increased the
80 efficiency of templated repair by 2- to 5-fold in cultured mammalian cells as well as germline
81 editing of *Caenorhabditis elegans,* zebrafish *(Danio rerio)* and mouse *(Mus musculus)*. The
82 modified donors exhibited a striking reduction in DNA ligation reactions including reduced self-
83 ligation into concatemers and reduced sequence-independent ligation into cellular DSBs,
84 suggesting that the 5′ modifications reduce the availability of 5′ ends for competing NHEJ
85 reactions.

86

87 # Results

88 **End-modified DNA donors increase the efficiencies of HDR in mammalian cells**

89 To examine the effects of donor end modifications on HDR in cultured mammalian cells, we took
90 advantage of a modified traffic light reporter (TLR) comprising a “broken” GFP coding region
91 followed by a frameshifted mCherry coding region [21, 22]. Cas9 targets the “broken” GFP, which
92 can only be made functional if precisely repaired by HDR, resulting in green fluorescence. If Cas9-
93 mediated DSBs are imprecisely repaired by NHEJ, approximately one third of the imprecise repair

events will restore the reading frame of mCherry, resulting in red fluorescence. Cas9 and single guide RNA (sgRNA) expression vectors and dsDNA donors with or without 5′ modifications were electroporated into HEK293T TLR cells (**Figure 1A)**, followed by flow cytometry to determine the percentage of cells expressing either GFP or mCherry.

We first examined the performance of dsDNA donors modified with 15-nucleotide (nt) 2′OMe-RNA fused to triethylene glycol (RNA::TEG). Strikingly, the frequency of HDR increased with the amount of RNA::TEG-modified donor to a maximal 52% GFP+ cells at 1.2 pmol of donor before falling off at higher amounts of donor (**Figure 1B**). By contrast, a maximum HDR frequency of only 25% GFP+ cells was observed at 1.6 pmol of unmodified donor. Notably, 0.4 pmol RNA::TEG-modified donor was as efficient as 1.6 pmol unmodified donor, suggesting that the modified donor is ~4-fold more potent than the unmodified donor (**Figure 1B**). The increase in GFP+ cells was accompanied by a corresponding reduction in mCherry+ cells (**Figure 1C**).

We reasoned that that the 2′O-Methyl RNA linker could be used to anneal PNA oligos attached to peptides that might enhance nuclear uptake. To test this idea, we produced complementary peptide-nucleic acid (PNA) oligos linked to a nuclear localization signal peptide or complementary PNA alone and tested these for HDR. Annealing these PNA oligos was well tolerated and did not diminish HDR, however neither did they enhance HDR (**Figure S1A-D**). Thus, further study will be needed to determine if RNA-TEG adapters can be used to append peptides or other molecules (e.g. CAS9 RNP) that stimulate HDR.

We next used the TLR assay to define features of the RNA::TEG moiety that promote maximal HDR. Nucleofection of 1.2 pmol donors modified with 2′OMe-RNA, TEG, or covalent RNA::TEG moieties all boosted HDR while reducing NHEJ events (**Figure 1D and E**). Increasing the length of the ethylene glycol moiety (3, 6, or 12 repeats) supported similar levels of HDR with

or without the 2′OMe-RNA moiety (**Figure 1F**). Finally, donors with TEG modification at both 5′ ends yielded slightly better HDR efficiencies than donors with modification at only one of the two 5′ ends (**Figure 1G**). However, donors with RNA::TEG modification at both 5′ ends or at only one of the 5′ ends yielded similar HDR efficiencies (**Figure 1G**).

To explore the utility of TEG- and RNA::TEG-modified donors for repair at other genomic loci, we generated donors to integrate full-length *eGFP* at the endogenous *TOMM20*, *GAPDH*, and *SEC61B* loci (**Figure 2A**). We found that TEG or RNA::TEG donors consistently exhibited increased HDR levels in HEK293T cells as measured by the fraction of cells expressing eGFP at *TOMM20* (2-fold), at *GAPDH* (3-fold), and at SEC61B (5-fold) when compared to unmodified dsDNA donor (**Figure 2B-D**). RNA::TEG-modified donors also substantially increased HDR in two cell types that are less amenable to editing, increasing HDR at the *TOMM20* locus in human foreskin fibroblasts (HFF) cells (2.3-fold) and at the *Gapdh* locus in Chinese hamster ovary (CHO) cells (6-fold) (**Figure 2E-F**).

Next, to quantify the nature of repair outcomes (precise and imprecise), we employed deep sequencing assays. To facilitate sequencing across the repair site, we replaced a 12-nt sequence with a 9-nt sequence at the *EMX1* locus in HEK293T. We compared HDR efficiencies in this assay using unmodified, TEG-modified, and RNA::TEG-modified dsDNA donors with 90-base pair (bp) homology arms (**Figure 2G**). At 1.2 pmol and 2.4 pmol, RNA::TEG modified donors yielded two fold more precise edits compared to the unmodified donors. When even higher doses (5pmol) were used, the gap in efficacy between unmodified and RNA::TEG modified donors narrowed to just 16% (89.5% vs 72.8%) precise reads (**Figure 2H**). The *EMX1* donor with 90-bp homology arms also supported high levels of HDR in K562 cells across a broad dose range. Notably, low doses of donor supported higher levels of HDR in K562 cells than in HEK293T cells, suggesting that K562

cells are more susceptible to editing (**Figure S2**). In this assay, donors modified with TEG alone exhibited no benefit over unmodified donors (**Figure 2H** and **Figure S2**).

5′-modification increases potency of single-stranded DNA donors

The experiments described thus far employed dsDNA donors; however, long single-stranded DNA (ssDNA) or short single-stranded oligo deoxynucleotide (ssODN) donors are also widely used in many HDR editing protocols. We therefore decided to explore how 5′ end modifications affect single stranded donors of different lengths. Using the TLR assay, we found that addition of RNA::TEG at the 5′ end of a long (800-nt) ssDNA donor significantly boosted HDR compared to the unmodified ssDNA donor. The frequency of HDR increased with the dose of ssDNA donor, reaching maximal HDR (22.5% GFP(+)cells) at 6 pmol to 8 pmol donor amounts (**Figure 3A, Figure S3A**). The RNA::TEG-modified donor was greater than 4-fold more potent than the unmodified donor reaching a threshold of 16% GFP(+) cells at a concentration of approximately 2 pmol whereas achieving the same threshold of 16% required 8 pmol of unmodified donor (**Figure 3A)**.

High yields of HDR in cultured mammalian cells have been achieved using short synthetic single-stranded oligo deoxynucleotide (ssODN) donors [23]. To test 5′-modified ssODNs for HDR efficacy, we used a sensitive GFP-to-BFP conversion assay in K562 cells. Precise editing converts a functional GFP sequence to blue fluorescent protein (BFP) sequence, producing cells that are GFP(-) and BFP(+). Imprecise editing produces cells that are both GFP(-) and BFP(-) [24]. Using 66 nt long ssODN donors and titrating the amount over a range of 0.01 to 40 pmol, we found that RNA::TEG and unmodified donors produced similar maximal levels of HDR (47.5% to 52.8% BFP(+) cells). However, maximal HDR required 10-fold less RNA::TEG-modified ssODN than

unmodified donors (**Figure 3B**). We also observed reduced levels of imprecise editing (GFP-negative and BFP-negative) as the frequency of HDR increased (**Figure S3B**). For both donor types, the decline in editing at higher doses correlated with the appearance of dead cells (data not shown), suggesting that dose-limiting toxicity scales with increased HDR potency.

The use of fully synthetic ssODN donors allowed us to explore additional modifications, including internal and 3′ modifications. Interestingly, 2′OMe-RNA, RNA::TEG, or TEG moieties at the 3′ terminus did not enhance HDR compared to unmodified ssODN, but they blocked the ability of 2′OMe-RNA, RNA::TEG, or TEG moieties at the 5′ end to enhance HDR (**Figure 3C, Figure S4**). By contrast, HDR was neither enhanced nor impeded by phosphorothioate (PS) linkages placed at 5′ or 3′ terminal linkages at the doses tested (**Figure S4)**. Taken together these findings suggest that the mechanism of HDR improvement requires an available 3′-OH.

5′-modified donors promote precision germline editing in *C. elegans*

Efficient genome editing in *C. elegans* can be achieved by directly injecting mixtures of Cas9 ribonucleoprotein (RNP) complex and donor into the syncytial ovary[25-27], producing dozens of independent precision editing events among the progeny of each injected animal [28]. We designed unmodified, TEG-modified, and RNA::TEG-modified donors to insert *gfp* at the *csr-1* locus or to correct *eft-3p::gfp* reporter that contains partial sequence of *gfp* (see Methods; **Figure 4A**). To monitor injection quality, we co-injected a plasmid encoding the transformation marker *rol-6(su1006)*, which produces the Roller phenotype. The TEG- and RNA::TEG-modified donors produced about twice as many GFP(+) progeny per injected animal than did the unmodified donor (**Figure 4B and E,** two representative broods per donor). Among the Roller cohort, which was previously shown to exhibit lower editing efficiency [28], end-modified donors increased the fraction

of GFP(+) Roller progeny by several fold. For example, whereas the unmodified *eft-3* donor produced only 12.6% GFP-positive Rollers, the TEG- and RNA::TEG-modified *eft-3* donors produced 57.1% and 49% GFP-positive Rollers (**Figure 4C**). Similarly, GFP::CSR-1(+) Rollers increased from 8.8% (unmodified) to 28% (TEG) and 32.8% (RNA::TEG) (**Figure 4F**). TEG- and RNA::TEG-modified *eft-3* and *csr-1* donors produced >50% GFP(+) non-Roller progeny compared to roughly 22% (*eft-3*) and 30% (*csr-1*) GFP(+) non-Rollers produced by the unmodified donor (**Figure 4D and G**). Every GFP(+) animal tested transmitted the edit to the next generation (**Figure S5A and B**). Thus, compared to the unmodified donors, the 5′-TEG and 5′-RNA::TEG donors substantially increase the frequency of *gfp* insertion by HDR in the *C. elegans* germline. Strikingly, end-modified donors frequently yielded more than 100 independent GFP(+) F1 progeny from a single injected hermaphrodite.

5′-modified donors promote precision editing in vertebrate zygotes

We next asked if donor 5′-modifications improve precision genome editing in zebrafish and mouse zygotes. For zebrafish genome editing, we designed 147-bp dsDNA donors to insert the 45-nt Avitag sequence into the 5′ end of the *Hey2* coding sequence (**Figure 5A**). Unmodified or end-modified donors were co-injected with Cas12a RNPs into one-cell embryos (see Methods), and editing efficiencies were quantified by high-throughput sequencing using genomic DNA isolated 24 hr after injection [29]. Strikingly, the frequency of precise editing was 11-fold higher with the RNA::TEG (4.4%) donor than with the unmodified donor (0.4%)(**Figure 5A**). The TEG-modified donor however failed to enhance precise editing in zebrafish zygotes (**Figure 5A**). The total level of editing was comparable in each condition as shown by the fraction of reads with indels (**Figure S6)**.

To test whether RNA::TEG-modified donors enhance precise editing in mouse zygotes, we targeted the *Tyrosinase (Tyr)* and *Sox2* loci. First, we sought to convert the coat color of Swiss-Webster albino (Tyr^{c}) mice to a pigmented phenotype ($Tyr^{c\text{-}cor}$*; cor: corrected)* using a donor to replace the serine 103 codon (TCT) with a cysteine (TGC) codon. The donor also introduces six silent mutations to prevent the guide RNA from directing cleavage of the edited locus (**Figure 5B**). We injected unmodified or RNA::TEG-modified donors with Cas9 RNPs into zygotes, transferred the embryos into pseudo-pregnant females, and quantified the repair efficiency by phenotyping the coat color of founder (F0) mice. The RNA::TEG-modified donor yielded more than twice as many pigmented F0 mice (37.9% uniform or mosaic) compared to unmodified donor (17.4%) (**Figure 5B, Figure S7A**). Strikingly, most (92%) of the edited founders produced by the RNA::TEG-modified donor had uniformly pigmented coats, whereas only 62.5% of the edited F0 produced by the unmodified donor had a uniformly pigmented coat color (**Figure 5C; Figure S7A**), suggesting that the RNA::TEG-modified donor promotes editing during early zygotic divisions. Representative images of F0 litters with dark coat color are shown in **Figure 5D**. We confirmed that F0 mice with pigmented coat transmitted the corrected $Tyr^{c\text{-}cor}$ allele to F1 pups (**Figure S7B and C**). Taken together, these results show that RNA::TEG donors are at least two-fold more efficient than unmodified donors in mouse zygote editing.

Next, we sought to insert a sequence encoding an in-frame V5 epitope immediately before the stop codon at the 3′ end of the *Sox2* locus (**Figure 5E**). We injected unmodified or RNA::TEG-modified donors with Cas9 RNPs into zygotes, transferred the embryos into pseudo-pregnant mice, and genotyped F0 progeny by PCR across the *Sox2* target site and Sanger sequencing. The V5 tag was precisely inserted into the *Sox2* locus in only 5.7% (n=35) of F0 animals from the injection with unmodified donor. By contrast, the RNA::TEG-modified donor resulted in precise insertion

of V5 in 33.3% (n=24) of the F0 animals—a greater than 5-fold increase in precise editing (**Figure 5E and Figure S8A**). All of the V5-positive founders tested (one F0 from the unmodified donor and six F0s from RNA::TEG-modified donor) transmitted the *Sox2::V5* allele to F1 progeny and the insertion was confirmed by Sanger sequencing (**Figure S8B** and **C**). Thus the 5′-RNA::TEG modification greatly improves the efficiency of precise genome editing in vertebrate model systems.

5′-modifications suppress donor concatenation

Upon delivery into animal cells or embryos, linear DNA molecules are known to form extensive homology-mediated and ligation-dependent concatemers (**Figure 6A**) [16-18]. We reasoned that 5′ modifications to the donor might suppress the formation of concatemers, thereby making linear donors more available for HDR. To test this idea, we nucleofected 566 bp dsDNA donors into HEK293T cells, harvested cells over a course of 3 days, and assessed the formation of concatemers by Southern blot analysis. We found that the unmodified dsDNA formed concatemers within 1 hour after nucleofection. These concatemers were composed of two to several copies of the DNA, inferred from the presence of a ladder of bands on the Southern blot (**Figure 6B**). Concatemers of up to ten copies were present within 3 hours after nucleofection and peaked in abundance by 12 hours. Concatemer levels declined over the next 12 hours but persisted at low levels until at least 72 hours after nucleofection. By contrast, the TEG-modified DNA showed a marked delay in the formation and levels of multimers (**Figure 6B**). Dimers and trimers gradually formed over the first 12 to 24 hours but were present at much lower levels than those formed by unmodified DNA. At late time points—24, 48, and 72 hours after transfection—we observed a greater fraction of TEG-

253 modified DNA monomers than unmodified monomers (**Figure 6B**). These results suggest that the
254 5′-TEG modification significantly suppresses concatemer formation.
255
256 ## End-modifications suppress direct ligation of short DNA into DSBs
257 To determine if TEG modification suppresses the direct ligation of TEG-modified linear molecules
258 into chromosomal DSBs, we performed GUIDE-seq analyses [30], which measures the incorporation
259 of short (34nt) dsDNA into on-target and off-target DSBs. We targeted the *ARHGEF9* locus,
260 previously characterized for off-target editing [31]. Strikingly, the TEG-modified DNA produced 19-
261 fold fewer GUIDE-seq reads (genome wide) than did the unmodified DNA (**Figure 6C)**. The
262 number of TEG-modified DNA insertions obtained at the on-target cut site in the *ARHGEF9* locus
263 and at the top 6 off target sites were dramatically reduced, ranging from 15-fold to 6-fold lower
264 compared to insertions of the unmodified DNA (**Figure 6D**). Taken together these data suggest
265 that TEG-modifications suppress direct ligation of donor molecules both to each other and to
266 chromosomal DSBs.
267
268 ## Discussion
269 Here we have explored how several types of chemical modifications to the repair template DNA
270 affect the efficiency of precise homology-dependent repair. In mammalian cells, donors containing
271 simple modifications such as TEG or 2′OMe-RNA::TEG on their 5′ ends improved HDR efficacy.
272 These modifications increased the potency of single- and double-stranded DNA (long and short)
273 donors, allowing efficient editing at significantly lower amounts. Modifying the ends of the donors
274 suppressed concatemer formation and significantly reduced random integration of short dsDNA at
275 chromosomal DSBs.

End modifications affected long and short donors differently in mammalian cells. On long donors end modification caused a ~2-to-5-fold increase in HDR frequency (total efficacy) compared to unmodified donors and did so without changing the donor concentration where efficacy reached its plateau. In contrast, on short donors end modifications did not increase the maximal efficacy of HDR, but instead dramatically reduced the amount of donor required to reach that maximal level. Put another way, long DNA donors exhibited both increased potency and maximal efficacy when modified, while short ssODN and dsDNA donors exhibited increased potency but no increase in maximal efficacy. This difference requires further study but could be explained if shorter donors and longer DNA donors experience different dose-limiting barriers. For example, the dose-limiting toxicity of ssODNs could be driven by total number of free DNA ends per cell, while longer molecules could encounter dose-limiting toxicity driven by total DNA mass. Consistent with this idea, unmodified long dsDNA donors begin to plateau in efficacy at nearly 4-fold more mass, but ~10-fold lower molar amounts than ssODNs. When end-modified, both types of donor exhibit similar maximal efficacy in the 1 to 2 pmol range.

RNA::TEG-modified donors significantly increased the levels of precision editing in three different model organisms (*C. elegans*, zebrafish, and mice). In all three animals, high HDR efficiencies were achieved using end-modified dsDNA donors, that in some cases approached efficiencies previously observed for ssODN donors [27, 32]. Importantly, precise insertions were obtained with relatively short homology arms. For example, in mouse zygote injections, we used donors with homology arms of less than 90 bp, similar to typical arm lengths used for ssODN donors [33] and at relatively low concentrations (1 ng/µl).

How do end-modifications help increase the efficacy of the donors? Our findings suggest that they do so, in part, by suppressing non-homologous end-joining reactions. In several systems

dsDNA donors have been shown to quickly form extrachromosomal arrays [16-18] and may do so directly in the cytoplasm [34]. For example, DNA delivered into the cytoplasm of the *C. elegans* gonadal syncytium gains entry into oocytes over a 24 hour period in a manner more consistent with cytoplasmic flow than with direct nuclear uptake by germ nuclei [28], and transformants established in this way have been shown to contain concatenated arrays of injected DNA, several hundred kilobases in length, which then partition to progeny in a non-Mendelian fashion as extrachromosomal elements [18, 35]. Integration of similar extrachromosomal arrays into the host genome have been reported in zebrafish and mouse zygotes [19, 20, 36]. Thus, the suppression of donor concatemer formation by 5′ modified donors could increase the effective molar amounts of donor available for precise repair of the target double strand break. Similarly, once in the nucleus, the suppression of direct ligation to chromosomal DNA through end-joining reactions could further increase precision repair. Perhaps consistent with suppression of concatenation as a major mechanism of action, it is intriguing that modification of a single end was nearly as effective as modifications to both ends of the donor. In principle, a single end modification would limit concatenation to dimer formation. Similarly, modification of a single end could prevent donors from ligating into circles which might then concatenate further through HDR.

In addition to increasing the amount of available donor molecules, another possible benefit of suppressing end-joining reactions is that the free ends of the donor might then be available to participate in the HDR mechanism (for example, by assembling elements of the DSB repair machinery directly on the free 3′-end of the donor). We found that a free unmodified 3′ end was required for efficient HDR. Thus, by suppressing ligation, the 5′ modification in effect maintains available 3′ ends, perhaps to prime repair synthesis.

In previous studies, fluorescent and amine modifications to the 5′ and 3′ termini of ssODN donors did not improve HDR efficacy over unmodified donors [37]. However, these studies were performed using doses 50-fold higher than the optimal dose for modified donors determined here. Similarly, phosphorothioate (PS) linkages were shown to improve HDR at doses much higher than the optimal dose for modified ssODNs in our study [4]. In our study, ssODNs with PS linkages did not improve HDR at doses where RNA::TEG- and TEG-modified donors were most efficacious. While our study was in preparation [38], three studies explored donors with 5′-end modifications. One study showed that the addition of biotin improved HDR and favored single copy insertion in the rice fish medaka [39]. The biotin moiety was attached to the donor via a polyethylene glycol (PEG) linker, but the study did not explore donors with PEG alone. Yu et al. (2020) showed that PEG10 with a 6-carbon linker boosted precise GFP insertions in vertebrate cells similar to those reported here for TEG- and RNA::TEG-modified donors, and at similar concentrations to those we employed [40]. The third study describes the suppression of NHEJ-mediated insertions using donors with 5′-Biotin::PEG or 5′-ssDNA::PEG moieties [41]. Our studies are in agreement with these findings and extend them to additional modifications and to *in vivo* genome-editing applications in three animal systems.

We do not understand why donors modified with TEG and RNA::TEG performed similarly in *C. elegans*, while RNA::TEG was consistently superior to TEG alone in zebrafish and human cells. The *C. elegans* system is unique in that it targets meiotic pachytene nuclei that are actively engaged in HDR. Perhaps donors must persist longer to engage the DSB repair machinery in mitotic cells. The RNA::TEG modification might therefore facilitate editing in mitotic cells by providing better protection from nuclease activity compared to TEG alone. PS linkages are known to protect against nuclease activity [4], and it will therefore be interesting to explore whether a

344 combination of internal (e.g., PS linkages) and terminal (e.g., 5′-RNA::TEG or 5′-TEG)
345 modifications can further increase HDR efficacy. Indeed, our results should incite the search for
346 additional chemistries that could boost donor stability while still allowing the donor to serve as a
347 template for repair polymerases; some such studies are underway in our laboratories. Future
348 studies will also need to explore whether the incorporation of donor chemistries will synergize
349 with other methods that stimulate HDR [1, 2, 14, 15, 42-44].

Acknowledgements. This work was funded by Howard Hughes Medical Institute (C.C.M.), NIH R37GM058800-23 (C.C.M), institutional funds from University of Massachusetts Medical School (E.J.S and J.K.W), NIH UG3 TR002668 (E.J.S and J.K.W), NIH/NHLBI R35 HL140017 (N.D.L) and NIH/OD R21 OD030004 (N.D.L). We thank Darryl Conte, Jr. for critical reading of the manuscript, Scot Wolfe for sharing the Cas9 expression plasmid, Julia Rembetsy-Brown for maintaining *Sox2::V5* mouse colony and Alireza Edraki for help with PCRs of some human dsDNA donors. Biorender was used to generate some of the graphics in figures. We thank the UMass Medical School Deep Sequencing Core for their assistance with the Illumina and PacBio sequencing.

Competing interests: The authors (K.S.G, A.M, G.A.D, H.G, J.K.W, E.J.S and C.C.M) have a patent application pending related to the findings described. Craig C. Mello is a co-founder and Scientific Advisory Board member of CRISPR Therapeutics, and Erik J. Sontheimer is a co-founder and Scientific Advisory Board member of Intellia Therapeutics.

References

1. Lin, S., Staahl, B.T., Alla, R.K. & Doudna, J.A. Enhanced homology-directed human genome engineering by controlled timing of CRISPR/Cas9 delivery. *Elife* **3**, e04766 (2014).
2. Wienert, B. et al. Timed inhibition of CDC7 increases CRISPR-Cas9 mediated templated repair. *Nat Commun* **11**, 2109 (2020).
3. Nambiar, T.S. et al. Stimulation of CRISPR-mediated homology-directed repair by an engineered RAD18 variant. *Nat Commun* **10**, 3395 (2019).
4. Renaud, J.B. et al. Improved Genome Editing Efficiency and Flexibility Using Modified Oligonucleotides with TALEN and CRISPR-Cas9 Nucleases. *Cell Rep* **14**, 2263-2272 (2016).
5. Rees, H.A., Yeh, W.H. & Liu, D.R. Development of hRad51-Cas9 nickase fusions that mediate HDR without double-stranded breaks. *Nat Commun* **10**, 2212 (2019).
6. Jayathilaka, K. et al. A chemical compound that stimulates the human homologous recombination protein RAD51. *Proc Natl Acad Sci U S A* **105**, 15848-15853 (2008).
7. Pinder, J., Salsman, J. & Dellaire, G. Nuclear domain 'knock-in' screen for the evaluation and identification of small molecule enhancers of CRISPR-based genome editing. *Nucleic Acids Res* **43**, 9379-9392 (2015).
8. Riesenberg, S. & Maricic, T. Targeting repair pathways with small molecules increases precise genome editing in pluripotent stem cells. *Nat Commun* **9**, 2164 (2018).
9. Yu, C. et al. Small molecules enhance CRISPR genome editing in pluripotent stem cells. *Cell Stem Cell* **16**, 142-147 (2015).
10. Canny, M.D. et al. Inhibition of 53BP1 favors homology-dependent DNA repair and increases CRISPR-Cas9 genome-editing efficiency. *Nat Biotechnol* **36**, 95-102 (2018).
11. Robert, F., Barbeau, M., Ethier, S., Dostie, J. & Pelletier, J. Pharmacological inhibition of DNA-PK stimulates Cas9-mediated genome editing. *Genome Med* **7**, 93 (2015).
12. Frank-Vaillant, M. & Marcand, S. Transient stability of DNA ends allows nonhomologous end joining to precede homologous recombination. *Mol Cell* **10**, 1189-1199 (2002).
13. Mao, Z., Bozzella, M., Seluanov, A. & Gorbunova, V. Comparison of nonhomologous end joining and homologous recombination in human cells. *DNA Repair (Amst)* **7**, 1765-1771 (2008).
14. Chu, V.T. et al. Increasing the efficiency of homology-directed repair for CRISPR-Cas9-induced precise gene editing in mammalian cells. *Nat Biotechnol* **33**, 543-548 (2015).
15. Maruyama, T. et al. Increasing the efficiency of precise genome editing with CRISPR-Cas9 by inhibition of nonhomologous end joining. *Nat Biotechnol* **33**, 538-542 (2015).
16. Perucho, M., Hanahan, D. & Wigler, M. Genetic and physical linkage of exogenous sequences in transformed cells. *Cell* **22**, 309-317 (1980).
17. Folger, K.R., Wong, E.A., Wahl, G. & Capecchi, M.R. Patterns of integration of DNA microinjected into cultured mammalian cells: evidence for homologous recombination between injected plasmid DNA molecules. *Mol Cell Biol* **2**, 1372-1387 (1982).
18. Mello, C.C., Kramer, J.M., Stinchcomb, D. & Ambros, V. Efficient gene transfer in C.elegans: extrachromosomal maintenance and integration of transforming sequences. *EMBO J* **10**, 3959-3970 (1991).

19. Stuart, G.W., McMurray, J.V. & Westerfield, M. Replication, integration and stable germ-line transmission of foreign sequences injected into early zebrafish embryos. *Development* **103**, 403-412 (1988).
20. Lacy, E., Roberts, S., Evans, E.P., Burtenshaw, M.D. & Costantini, F.D. A foreign beta-globin gene in transgenic mice: integration at abnormal chromosomal positions and expression in inappropriate tissues. *Cell* **34**, 343-358 (1983).
21. Certo, M.T. et al. Tracking genome engineering outcome at individual DNA breakpoints. *Nat Methods* **8**, 671-676 (2011).
22. Iyer, S. et al. Efficient Homology-directed Repair with Circular ssDNA Donors. *bioRxiv*, 864199 (2019).
23. Richardson, C.D., Ray, G.J., DeWitt, M.A., Curie, G.L. & Corn, J.E. Enhancing homology-directed genome editing by catalytically active and inactive CRISPR-Cas9 using asymmetric donor DNA. *Nat Biotechnol* **34**, 339-344 (2016).
24. Glaser, A., McColl, B. & Vadolas, J. GFP to BFP Conversion: A Versatile Assay for the Quantification of CRISPR/Cas9-mediated Genome Editing. *Mol Ther Nucleic Acids* **5**, e334 (2016).
25. Cho, S.W., Lee, J., Carroll, D., Kim, J.S. & Lee, J. Heritable gene knockout in Caenorhabditis elegans by direct injection of Cas9-sgRNA ribonucleoproteins. *Genetics* **195**, 1177-1180 (2013).
26. Paix, A., Folkmann, A., Rasoloson, D. & Seydoux, G. High Efficiency, Homology-Directed Genome Editing in Caenorhabditis elegans Using CRISPR-Cas9 Ribonucleoprotein Complexes. *Genetics* **201**, 47-54 (2015).
27. Dokshin, G.A., Ghanta, K.S., Piscopo, K.M. & Mello, C.C. Robust Genome Editing with Short Single-Stranded and Long, Partially Single-Stranded DNA Donors in Caenorhabditis elegans. *Genetics* **210**, 781-787 (2018).
28. Ghanta, K.S. & Mello, C.C. Melting dsDNA Donor Molecules Greatly Improves Precision Genome Editing in Caenorhabditis elegans. *Genetics* **216**, 643-650 (2020).
29. Liu, P. et al. Enhanced Cas12a editing in mammalian cells and zebrafish. *Nucleic Acids Res* **47**, 4169-4180 (2019).
30. Tsai, S.Q. et al. GUIDE-seq enables genome-wide profiling of off-target cleavage by CRISPR-Cas nucleases. *Nat Biotechnol* **33**, 187-197 (2015).
31. Amrani, N. et al. NmeCas9 is an intrinsically high-fidelity genome-editing platform. *Genome Biol* **19**, 214 (2018).
32. Kan, Y., Ruis, B., Takasugi, T. & Hendrickson, E.A. Mechanisms of precise genome editing using oligonucleotide donors. *Genome Res* **27**, 1099-1111 (2017).
33. Quadros, R.M. et al. Easi-CRISPR: a robust method for one-step generation of mice carrying conditional and insertion alleles using long ssDNA donors and CRISPR ribonucleoproteins. *Genome Biol* **18**, 92 (2017).
34. Forbes, D.J., Kirschner, M.W. & Newport, J.W. Spontaneous formation of nucleus-like structures around bacteriophage DNA microinjected into Xenopus eggs. *Cell* **34**, 13-23 (1983).
35. Stinchcomb, D.T., Shaw, J.E., Carr, S.H. & Hirsh, D. Extrachromosomal DNA transformation of Caenorhabditis elegans. *Mol Cell Biol* **5**, 3484-3496 (1985).
36. Costantini, F. & Lacy, E. Introduction of a rabbit beta-globin gene into the mouse germ line. *Nature* **294**, 92-94 (1981).

37. Lee, K. et al. Synthetically modified guide RNA and donor DNA are a versatile platform for CRISPR-Cas9 engineering. *Elife* **6** (2017).
38. Ghanta, K.S. et al. 5′ Modifications Improve Potency and Efficacy of DNA Donors for Precision Genome Editing. *bioRxiv*, 354480 (2018).
39. Gutierrez-Triana, J.A. et al. Efficient single-copy HDR by 5' modified long dsDNA donors. *Elife* **7** (2018).
40. Yu, Y. et al. An efficient gene knock-in strategy using 5'-modified double-stranded DNA donors with short homology arms. *Nat Chem Biol* **16**, 387-390 (2020).
41. Canaj, H. et al. Deep profiling reveals substantial heterogeneity of integration outcomes in CRISPR knock-in experiments. *bioRxiv*, 841098 (2019).
42. Gutschner, T., Haemmerle, M., Genovese, G., Draetta, G.F. & Chin, L. Post-translational Regulation of Cas9 during G1 Enhances Homology-Directed Repair. *Cell Rep* **14**, 1555-1566 (2016).
43. Yang, D. et al. Enrichment of G2/M cell cycle phase in human pluripotent stem cells enhances HDR-mediated gene repair with customizable endonucleases. *Sci Rep* **6**, 21264 (2016).
44. Ling, X. et al. Improving the efficiency of precise genome editing with site-specific Cas9-oligonucleotide conjugates. *Sci Adv* **6**, eaaz0051 (2020).

Figure Legends

Figure 1. 5′ end-modified donors promote HDR in Traffic-Light Reporter (TLR) cells. (A) Schematic showing the TLR assay to quantify HDR efficiencies using unmodified or end-modified dsDNA donors. Editing efficiencies plotted as percentage of (B) GFP+ (HDR) and (C) mCherry+ (NHEJ) HEK293T TLR cells at different amounts of unmodified, 2′OMe-RNA::TEG-modified dsDNA donors. Editing efficiencies plotted as percentage of (D) GFP+ (HDR) and (E) mCherry+ (NHEJ) HEK293T TLR cells at 1.2 pmol of dsDNA donors indicated. Percentage of GFP+ cells obtained with dsDNA donors modified with various lengths of ethylene glycol (F) and with modifications to only one end or both5′ ends of the donor. TS- target strand, NTS- non-target strand (G). Mean ± s.d for at least three independent replicates are plotted; two replicates for TEG-donor in panel G.

Figure 2. End-modified donors promote HDR at endogenous loci in mammalian cell cultures. (A) schematic representation of the 5′ modified donor design for eGFP insertion and FACS sorting is shown. Efficacy of eGFP integration at (B) *TOMM20* and (C) *GAPDH* (D) Sec61B loci in HEK293T cells using unmodified, TEG or 2′OMe-RNA::TEG-modified donors are plotted as percentage of GFP+ cells. Efficacy of eGFP integration at the (E) *TOMM20* locus in HFF (747 bp knock-in with ~1kb homology arms) and (F) *Gapdh* locus in CHO (1635 bp knock-in with ~800 bp homology arms) cells using dsDNA (500 ng) donors with and without 2′OMe-RNA::TEG modifications at the 5′ ends. (G) Schematic representation of the dsDNA donor design used for quantification with deep sequencing is shown. (H) Illumina sequencing reads with precise knock-in are plotted for dsDNA donors with 90bp homology arms at EMX1 locus in HEK293T cells. Mean ± s.d for at least three independent replicates are plotted. P-values were calculated using

494 one-way ANOVA and in all cases end-modified donors were compared to unmodified donor
495 unless indicated otherwise (Tukey's multiple comparisons test; ****P < 0.0001; ***P < 0.001;
496 **P < 0.01; *P< 0.05; ns- not significant).
497
498 **Figure 3.** End-modifications increase potency of ssODN donors (A) Editing efficacy plotted as
499 percentage of GFP+ (precise) HEK293T TLR cells at different amounts of unmodified and 2′OMe-
500 RNA::TEG-modified long ssDNA donors (800 nt). (B) Editing efficacy of GFP-to-BFP reporter
501 conversion in K562 cells using different amounts of unmodified and 2′OMe-RNA::TEG-modified
502 66 nt ssODN donors plotted as percentage of BFP+ cells (HDR). (C). Editing efficacy of GFP-to-
503 BFP conversion in K562 cells using 0.5 pmol of ssODN donors modified at the 5′ end alone, the
504 3′ end alone, or at both the 5′ and 3′ ends, with phosphorothioate (PS), TEG, 2′OMe-RNA, or
505 2′OMe-RNA::TEG, plotted as percentage of BFP+ cells (precise). Complete figure of panel C is
506 shown, along with other modifications, in Figure. S4. Mean ± s.d for at least three independent
507 replicates are plotted. P-values were calculated using one-way ANOVA and in all cases end-
508 modified donors were compared to unmodified donor unless indicated otherwise (Tukey's multiple
509 comparisons test; ****P < 0.0001; ***P < 0.001; **P < 0.01; *P< 0.05; ns- not significant).
510
511 **Figure 4.** Modified donors promote precise editing in *C. elegans.* (A) Schematic showing end-
512 modified dsDNA donors (25ng/µl) with short (~35bp) homology arms to insert *gfp* tag. (B)
513 Number of GFP expressing animals among entire F1 brood of two representative P0 animals for
514 each donor type are plotted for *eft-3p* reporter locus. Fraction of F1 animals expressing GFP among
515 (C) Roller and (D) non-Roller cohorts are plotted as percentage for *eft-3p* locus. Similarly, (E)
516 number of GFP expressing animals among two representative broods, fraction of F1 animals

517 expressing GFP among (F) Roller and (G) non-Roller cohorts are plotted for *csr-1* locus. Open
518 bars (Rollers) and closed bars represent (non-Rollers) median. Number of GFP expressing animals
519 among total number of animals scored per cohort are shown above the bars. n ≥4 broods for each
520 donor condition. P-values were calculated using one-way ANOVA and in all cases end-modified
521 donors were compared to unmodified donors (Tukey's multiple comparisons test; ****P < 0.0001;
522 ***P < 0.001; **P < 0.01; *P< 0.05; ns- not significant).
523
524 **Figure 5.** 2′-OMe-RNA-TEG donors promote precise editing in vertebrate zygotes. (A)
525 unmodified, TEG and 2′-OMe-RNA-TEG modified dsDNA donors were injected into zebrafish
526 zygotes. dsDNA donor design to knock-in Avi-tag is shown on the top and the fraction of Illumina
527 reads containing precise knock-in are plotted as percentages. Mean ± s.d for at least three
528 independent replicates (two for unmodified donors) are plotted (B). Design of the dsDNA donors
529 injected into mouse zygotes to precisely convert the coat color of albino mice (Tyr^{C}) to pigmented
530 ($Tyr^{C\text{-}Cor}$) by editing C to G (underscored) along with six silent mutations (in red) is shown.
531 Percentages of F0 founder mice with black coat are shown. (C) percentages of animals among
532 HDR positive F0s that have uniform dark coat or mosaic coat color are plotted for unmodified and
533 5′ modified donors. (D) Representative pictures of 10 days old F0 mice with pigmented (HDR) or
534 white (wt or indel) coat color are shown. One mosaic mouse (third from left) can be seen among
535 the pups obtained with end-modified donor. (E) Donor design to knock-in V5 tag at the C-terminus
536 of Sox2 is shown on the top. Percentage of founder animals containing perfect *V5* insertion at *Sox2*
537 locus are shown for each donor type. HA: Homology Arms. P-values were calculated using one-
538 way ANOVA (Tukey's multiple comparisons test; ****P < 0.0001; ***P < 0.001; **P < 0.01;
539 *P< 0.05; ns- not significant).

Figure 6. End-modifications suppress formation of donor concatemers. (A) Model for mechanisms of concatemer formation is shown. (B) Southern blot of unmodified and TEG modified dsDNA (566bp) nucleofected into HEK293T cells and collected at indicated time points. Concatemerization of unmodified DNA is visualized as ladders; 566bp DNA and 13kb long DNA are used as size markers (m). Number of Guide-seq reads with unmodified and TEG modified short dsDNA (34bp) integration for, (C) whole genome and (D) on-target (*ARHGEF9)* and six previously validated off-target loci are plotted. Data from two biological replicates is shown.

Figure 1

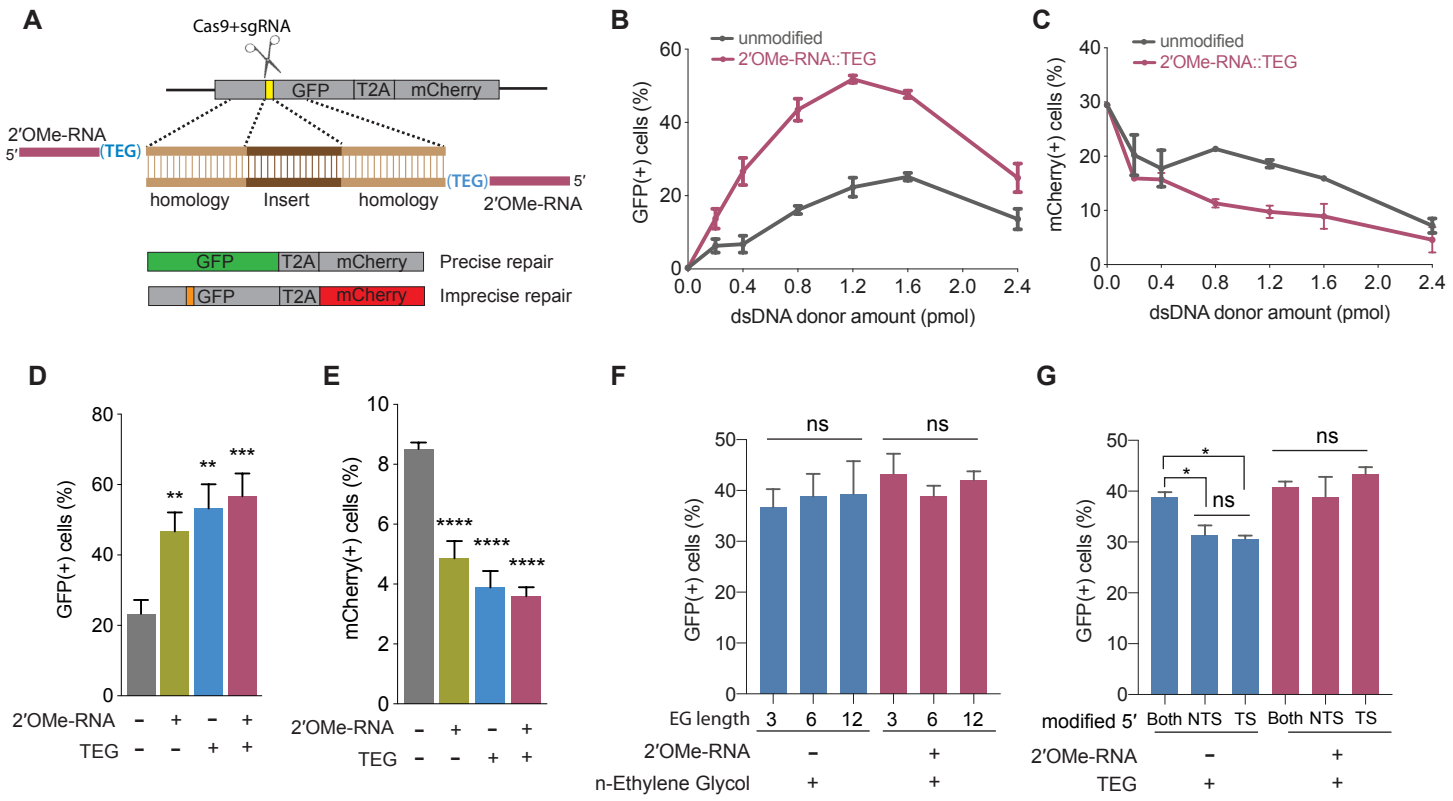

Figure 1. 5′ end-modified donors promote HDR in Traffic-Light Reporter (TLR) cells. (A) Schematic showing the TLR assay to quantify HDR efficiencies using unmodified or end-modified dsDNA donors. Editing efficiencies plotted as percentage of (B) GFP+ (HDR) and (C) mCherry+ (NHEJ) HEK293T TLR cells at different amounts of unmodified, 2′OMe-RNA::TEG-modified dsDNA donors. Editing efficiencies plotted as percentage of (D) GFP+ (HDR) and (E) mCherry+ (NHEJ) HEK293T TLR cells at 1.2 pmol of dsDNA donors indicated. Percentage of GFP+ cells obtained with dsDNA donors modified with various lengths of ethylene glycol (F) and with modifications to only one end or both5′ ends of the donor. TS- target strand, NTS- non-target strand (G). Mean ± s.d for at least three independent replicates are plotted; two replicates for TEG-donor in panel G

Figure 2

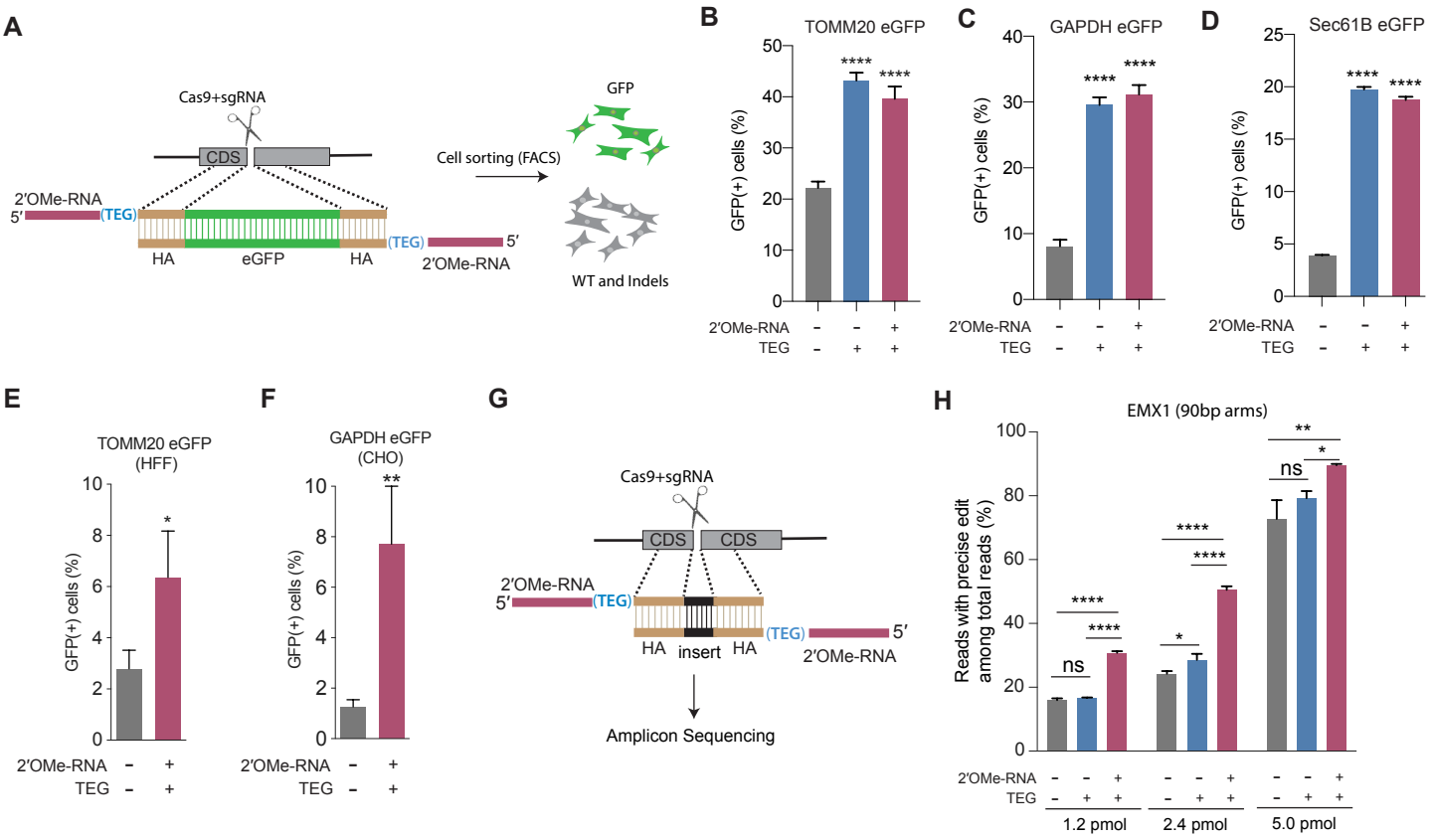

Figure 2. End-modified donors promote HDR at endogenous loci in mammalian cell cultures. (A) schematic representation of the 5′ modified donor design for eGFP insertion and FACS sorting is shown. Efficacy of eGFP integration at (B) TOMM20 and (C) GAPDH (D) Sec61B loci in HEK293T cells using unmodified, TEG or 2′OMe-RNA::TEG-modified donors are plotted as percentage of GFP+ cells. Efficacy of eGFP integration at the (E) TOMM20 locus in HFF (747 bp knock-in with ~1kb homology arms) and (F) Gapdh locus in CHO (1635 bp knock-in with ~800 bp homology arms) cells using dsDNA (500 ng) donors with and without 2′OMe-RNA::TEG modifications at the 5′ ends. (G) Schematic representation of the dsDNA donor design used for quantification with deep sequencing is shown. (H) Illumina sequencing reads with precise knock-in are plotted for dsDNA donors with 90bp homology arms at EMX1 locus in HEK293T cells. Mean ± s.d for at least three independent replicates are plotted. P-values were calculated using one-way ANOVA and in all cases end-modified donors were compared to unmodified donor unless indicated otherwise (Tukey's multiple comparisons test; ****P < 0.0001; ***P < 0.001; **P < 0.01; *P< 0.05; ns- not significant).

Figure 3

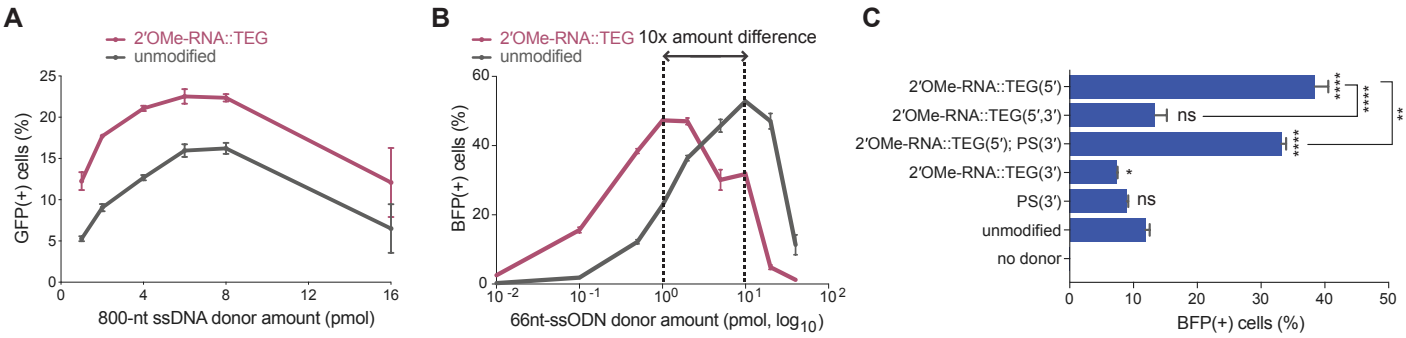

Figure 3. End-modifications increase potency of ssODN donors (A) Editing efficacy plotted as percentage of GFP+ (precise) HEK293T TLR cells at different amounts of unmodified and 2′OMe-RNA::TEG-modified long ssDNA donors (800 nt). (B) Editing efficacy of GFP-to-BFP reporter conversion in K562 cells using different amounts of unmodified and 2′OMe-RNA::TEG-modified 66 nt ssODN donors plotted as percentage of BFP+ cells (HDR). (C). Editing efficacy of GFP-to-BFP conversion in K562 cells using 0.5 pmol of ssODN donors modified at the 5′ end alone, the 3′ end alone, or at both the 5′ and 3′ ends, with phosphorothioate (PS), TEG, 2′OMe-RNA, or 2′OMe-RNA::TEG, plotted as percentage of BFP+ cells (precise). Complete figure of panel C is shown, along with other modifications, in Figure. S4. Mean ± s.d for at least three independent replicates are plotted. P-values were calculated using one-way ANOVA and in all cases end-modified donors were compared to unmodified donor unless indicated otherwise (Tukey's multiple comparisons test; ****P < 0.0001; ***P < 0.001; **P < 0.01; *P< 0.05; ns- not significant).

Figure 4

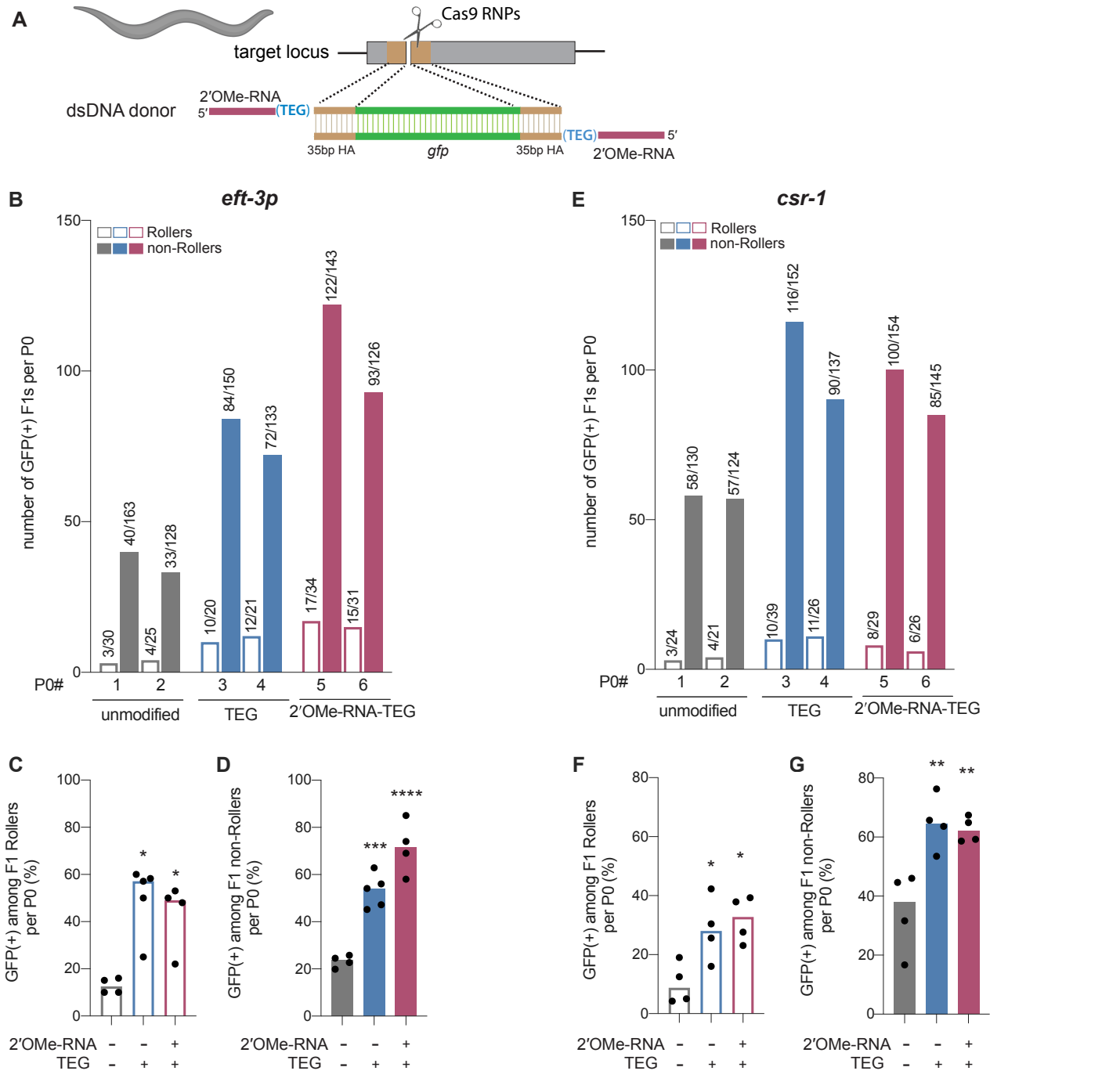

Figure 4. Modified donors promote precise editing in *C. elegans*. (A) Schematic showing end-modified dsDNA donors (25ng/µl) with short (~35bp) homology arms to insert gfp tag. (B) Number of GFP expressing animals among entire F1 brood of two representative P0 animals for each donor type are plotted for *eft-3p* reporter locus. Fraction of F1 animals expressing GFP among (C) Roller and (D) non-Roller cohorts are plotted as percentage for *eft-3p* locus. Similarly, (E) number of GFP expressing animals among two representative broods, fraction of F1 animals expressing GFP among (F) Roller and (G) non-Roller cohorts are plotted for *csr-1* locus. Open bars (Rollers) and closed bars represent (non-Rollers) median. Number of GFP expressing animals among total number of animals scored per cohort are shown above the bars. n ≥4 broods for each donor condition. P-values were calculated using one-way ANOVA and in all cases end-modified donors were compared to unmodified donors (Tukey's multiple comparisons test; ****P < 0.0001; ***P < 0.001; **P < 0.01; *P< 0.05; ns- not significant).

Figure 5

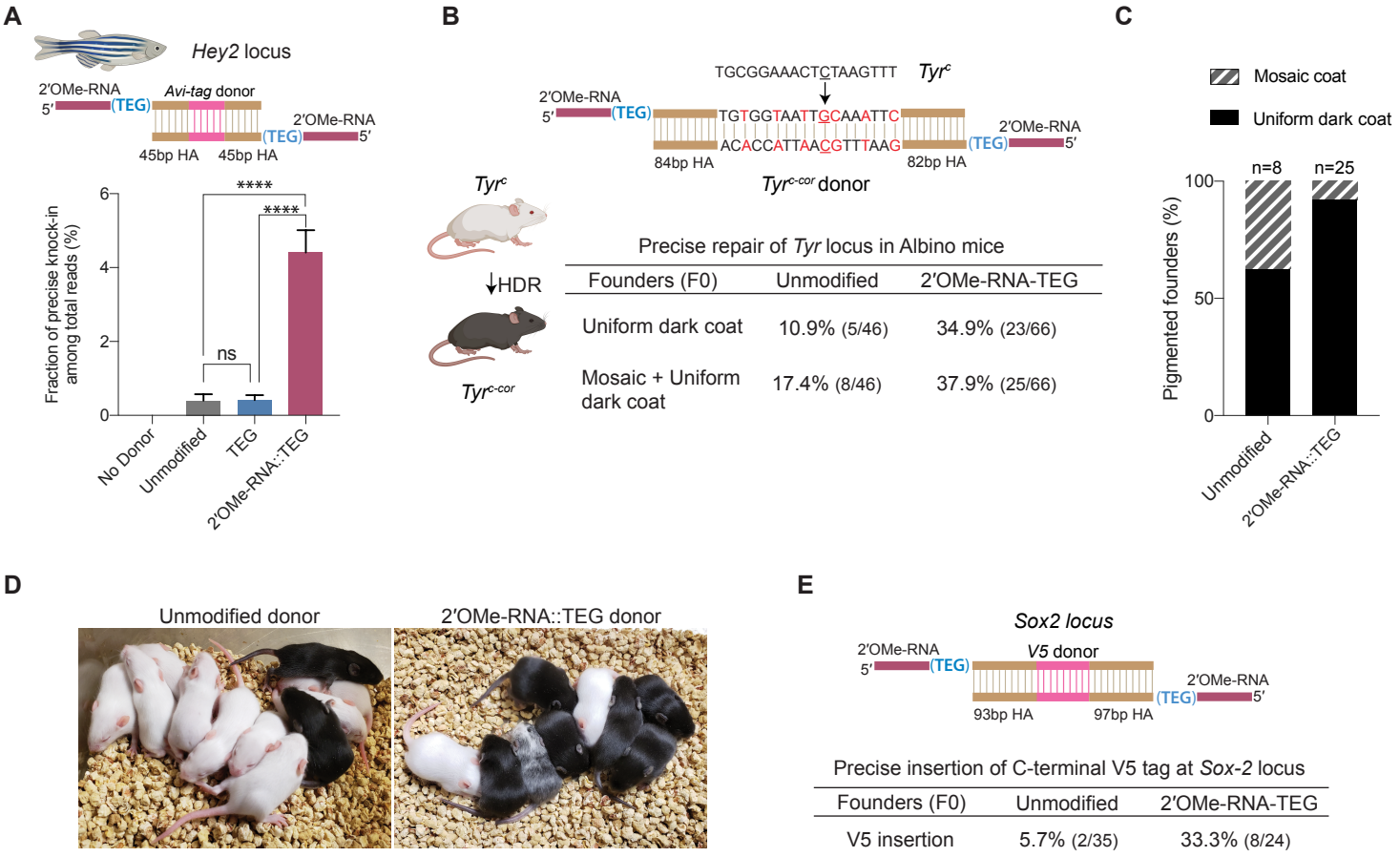

Figure 5. 2′-OMe-RNA-TEG donors promote precise editing in vertebrate zygotes. (A) unmodified, TEG and 2′-OMe-RNA-TEG modified dsDNA donors were injected into zebrafish zygotes. dsDNA donor design to knock-in Avi-tag is shown on the top and the fraction of Illumina reads containing precise knock-in are plotted as percentages. Mean ± s.d for at least three independent replicates (two for unmodified donors) are plotted (B). Design of the dsDNA donors injected into mouse zygotes to precisely convert the coat color of albino mice (*Tyr*^{C}) to pigmented (*Tyr*$^{C\text{-}Cor}$) by editing C to G (underscored) along with six silent mutations (in red) is shown. Percentages of F0 founder mice with black coat are shown. (C) percentages of animals among HDR positive F0s that have uniform dark coat or mosaic coat color are plotted for unmodified and 5′ modified donors. (D) Representative pictures of 10 days old F0 mice with pigmented (HDR) or white (wt or indel) coat color are shown. One mosaic mouse (third from left) can be seen among the pups obtained with end-modified donor. (E) Donor design to knock-in V5 tag at the C-terminus of Sox2 is shown on the top. Percentage of founder animals containing perfect V5 insertion at *Sox2* locus are shown for each donor type. HA: Homology Arms. P-values were calculated using one-way ANOVA (Tukey's multiple comparisons test; ****P < 0.0001; ***P < 0.001; **P < 0.01; *P< 0.05; ns- not significant).

Figure 6

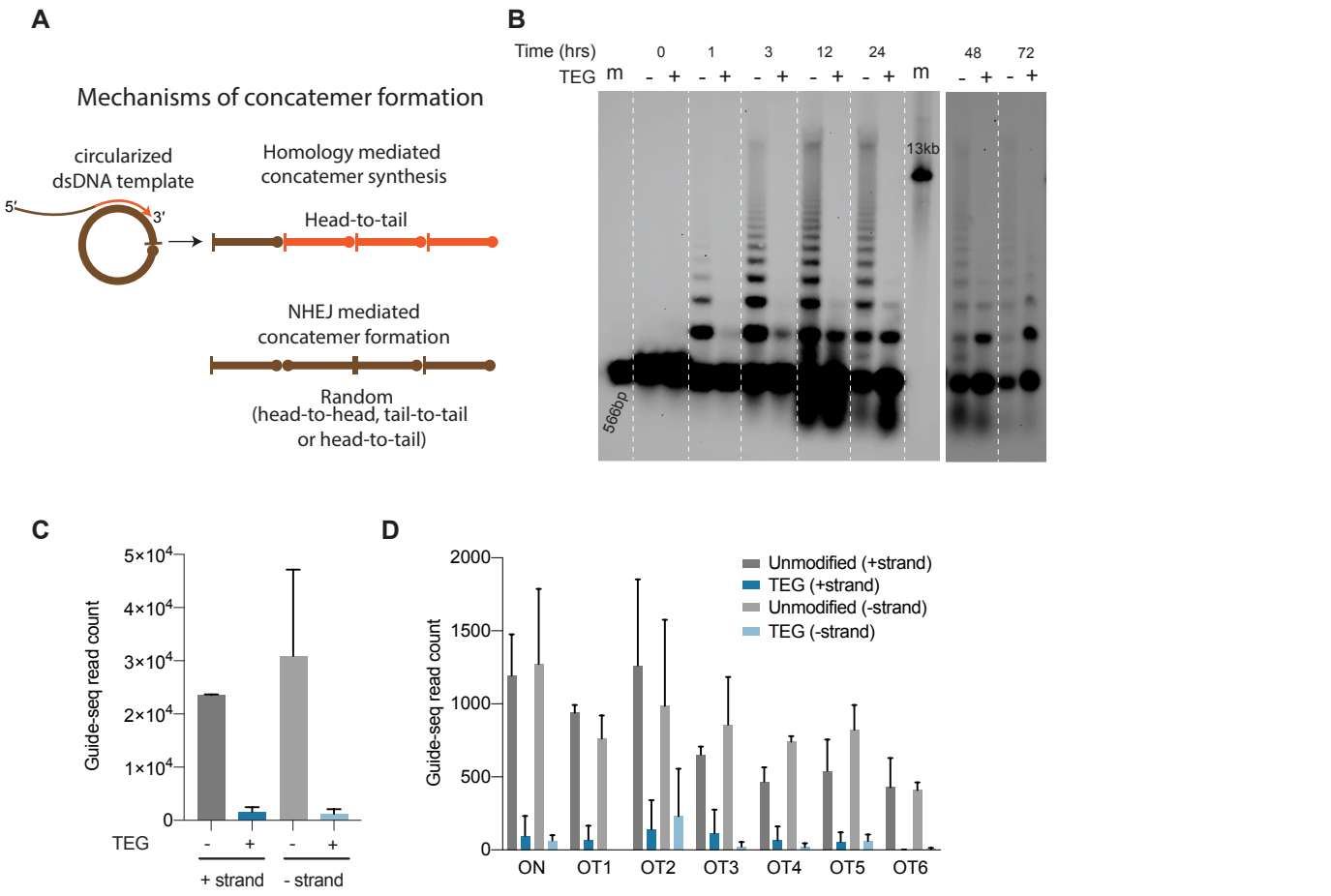

Figure 6. End-modifications suppress formation of donor concatemers. (A) Model for mechanisms of concatemer formation is shown. (B) Southern blot of unmodified and TEG modified dsDNA (566bp) nucleofected into HEK293T cells and collected at indicated time points. Concatemerization of unmodified DNA is visualized as ladders; 566bp DNA and 13kb long DNA are used as size markers (m). Number of Guide-seq reads with unmodified and TEG modified short dsDNA (34bp) integration for, (C) whole genome and (D) on-target (*ARHGEF9*) and six previously validated off-target(OT) loci are plotted; data from two biological replicates is shown.

Supplementary Materials for

5′ Modifications Improve Potency and Efficacy of DNA Donors for Precision Genome Editing

This PDF file includes:

Supplementary Figures. 1 to 9

Materials and Methods

Figure S1

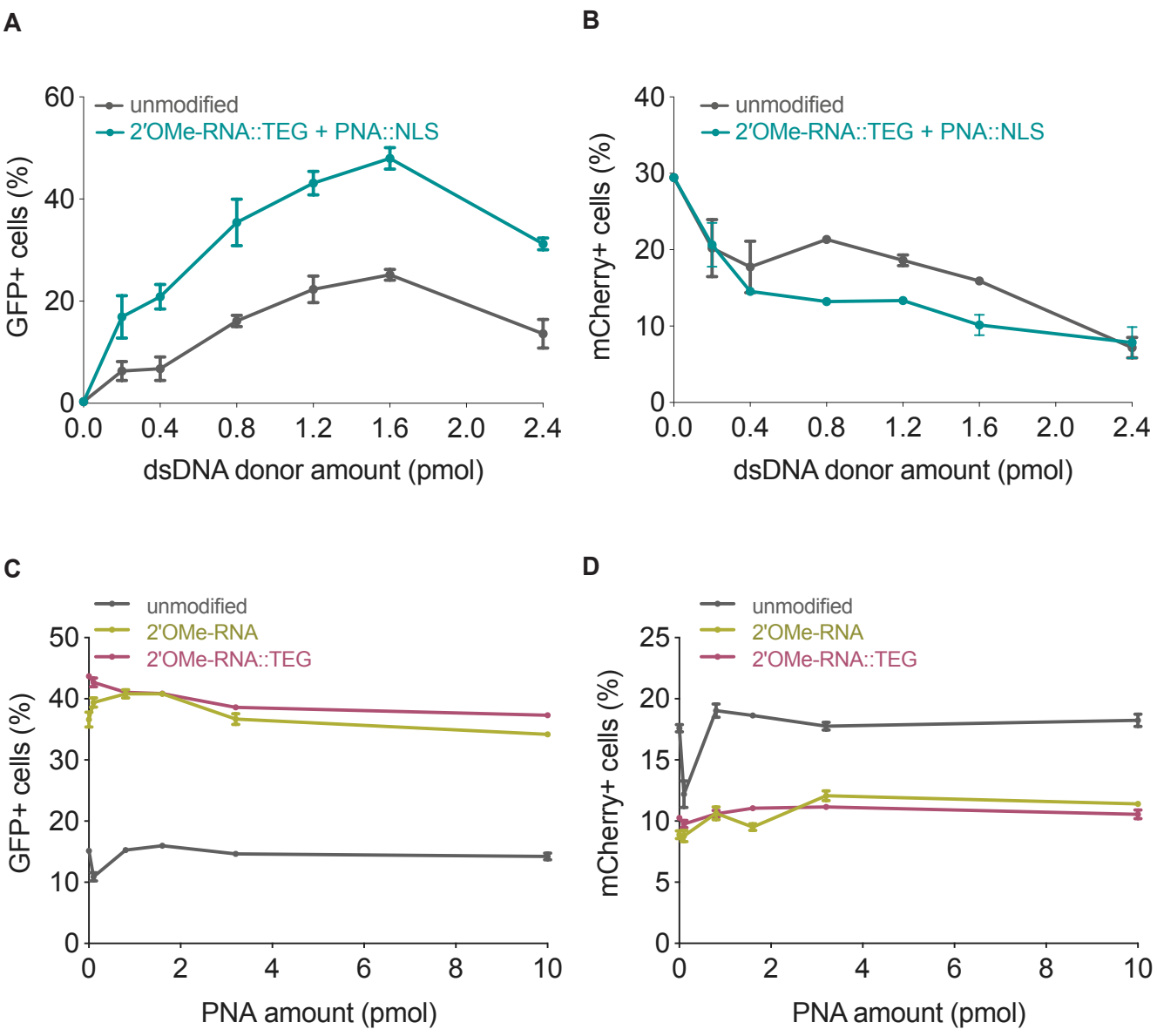

Figure S1: 2′OMe-RNA at 5′ ends of donors promote HDR in mammalian cells. Editing efficacy plotted as percentage of (A) GFP+ (HDR) and (B) mCherry+ (NHEJ) HEK293T TLR cells at different amounts of unmodified, 2′OMe-RNA::TEG-modified and PNA::NLS-annealed dsDNA donors. Same unmodified controls are used in Figure 1 B and C. Addition of PNA (without NLS) to unmodified or end-modified donors does not further improve HDR efficiency in mammalian cells. 0.8 pmol of each type of donor was annealed to PNA (0.1 to 10 pmol). Editing efficiency was plotted as percentage of (C) GFP+ (HDR) cells and (D) mCherry+ (NHEJ) cells. Percentages were calculated by sorting the cells through flow cytometry (see Methods)

Figure S2

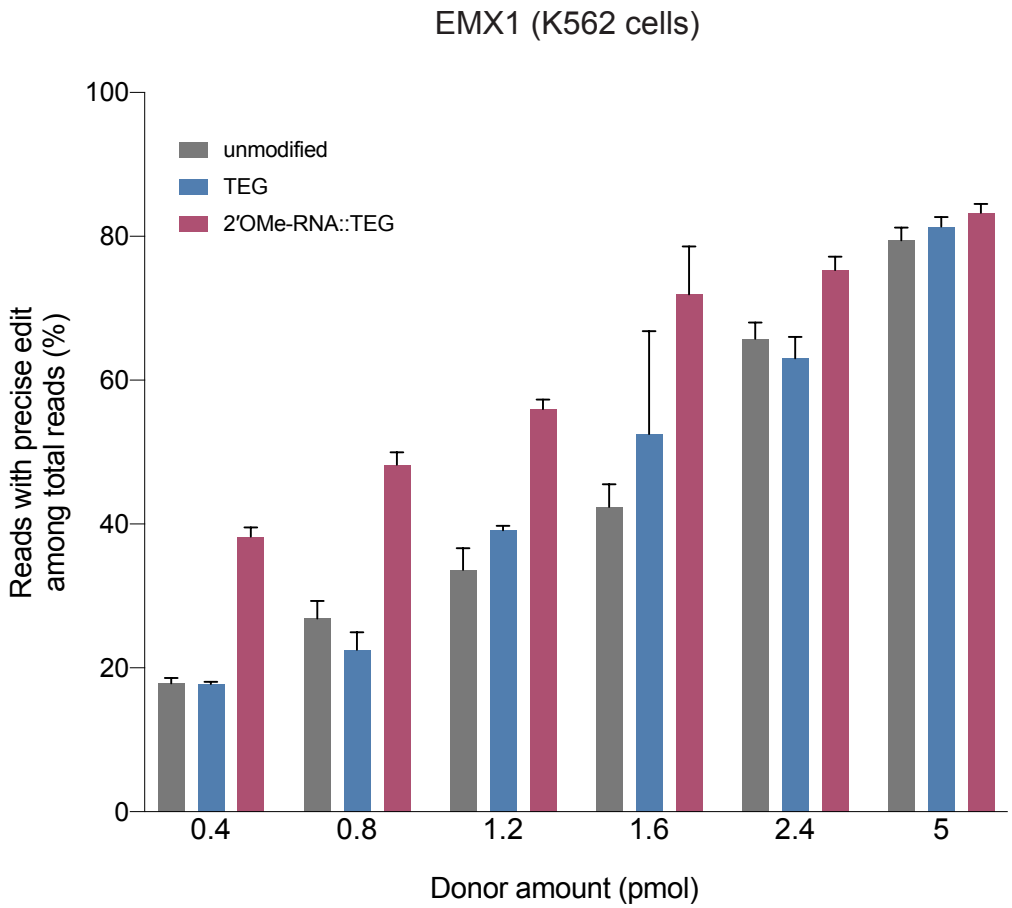

Figure S2. RNA::TEG donors with short (90bp) homology arms are more potent than unmodified donors at *EMX1* locus. Fraction of precise reads is plotted as percentage of total Illumina reads obtained at various amounts of dsDNA donors into K562 cells. Cas9 RNPs and dsDNA donors were nucleofected into K562 cells and harvested after 3 days.

Figure S3

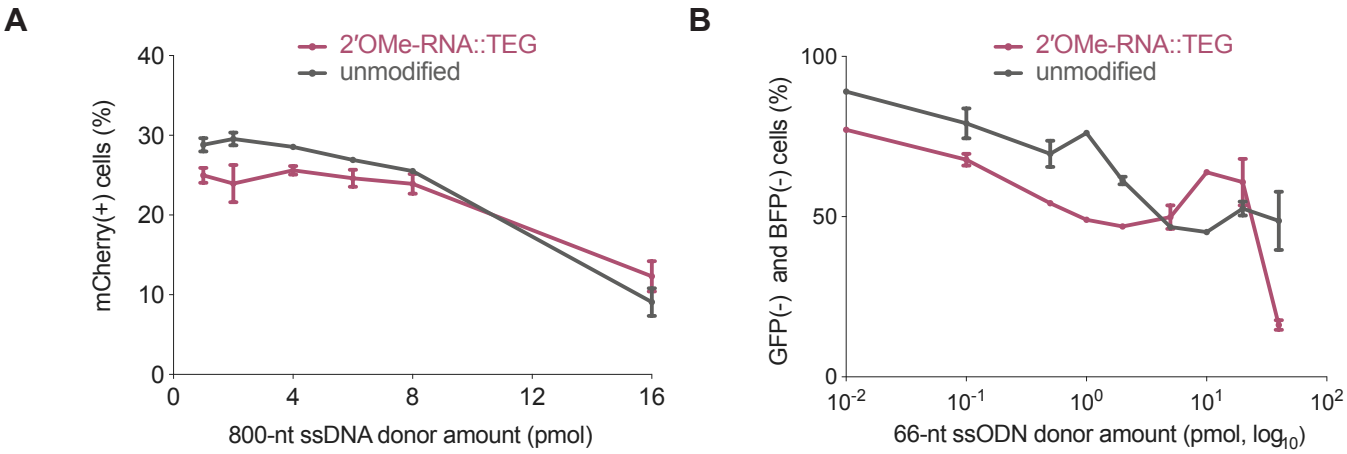

Figure S3. 2′OMe-RNA::TEG modification of single-stranded DNA donors results in reduced imprecise editing. (A) Imprecise editing efficiency plotted as percentage of mCherry(+)HEK293T TLR cells at different amounts of unmodified or TEG::2′OMe-RNA-modified ssDNA donor. Fraction of cells expressing GFP is plotted in Figure. 3A. (B) Imprecise editing plotted as percentage of GFP(-) and BFP(-) cells in GFP-to-BFP reporter K562 cells using different amounts of unmodified and TEG::2′OMe-RNA-modifed ssODN donors. Fraction of cells expresing BFP is plotted in Figure. 3B

Figure S4

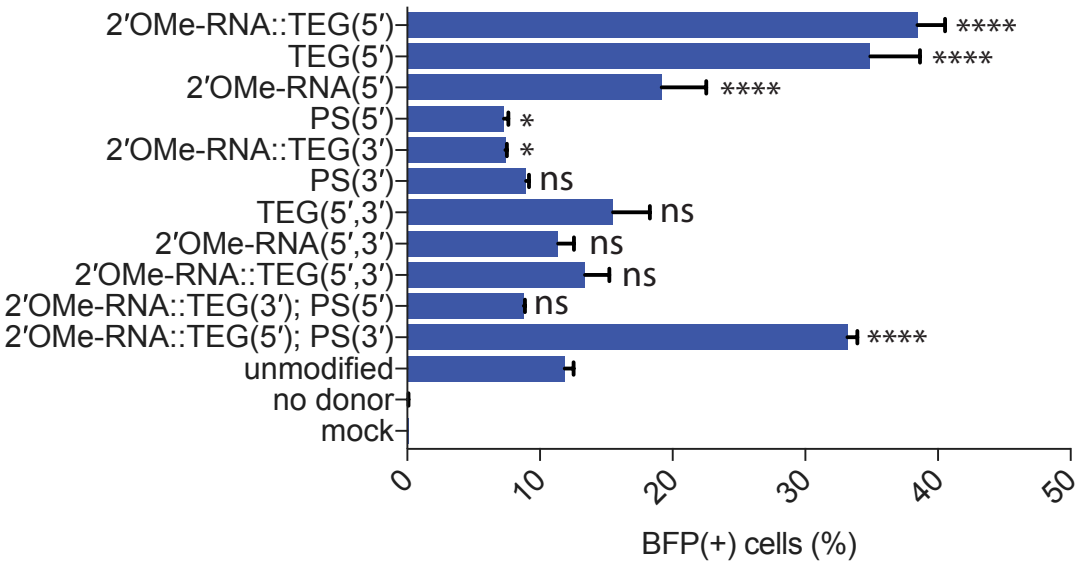

Figure S4. Effects of terminal and non-terminal modifications of ssODN donors on HDR efficacy. Editing efficacy of GFP-to-BFP conversion in K562 cells using 0.5 pmol of ssODN donors modified at the 5′ end alone, the 3′ end alone, or at both the 5′ and 3′ ends, with phosphorothioate (PS), TEG, 2′OMe-RNA, or 2′OMe-RNA::TEG, plotted as percentage of BFP(+) cells (HDR). This figure consists of the data shown in Figure. 3C along with other controls and modifications to the donors. Note that the PS modification is at the 5′ or 3′ internal linkages while TEG modifications are appended to the 5′ or 3′ terminus. All data points represent a mean of at least three independent replicates and all error bars represent standard deviation. P-values were calculated using one-way ANOVA and in all cases end-modified donors were compared to the unmodified donor (Tukey's multiple comparisons test; ****P < 0.0001; ***P < 0.001; **P < 0.01; *P< 0.05; ns- not significant).

Figure S5

A

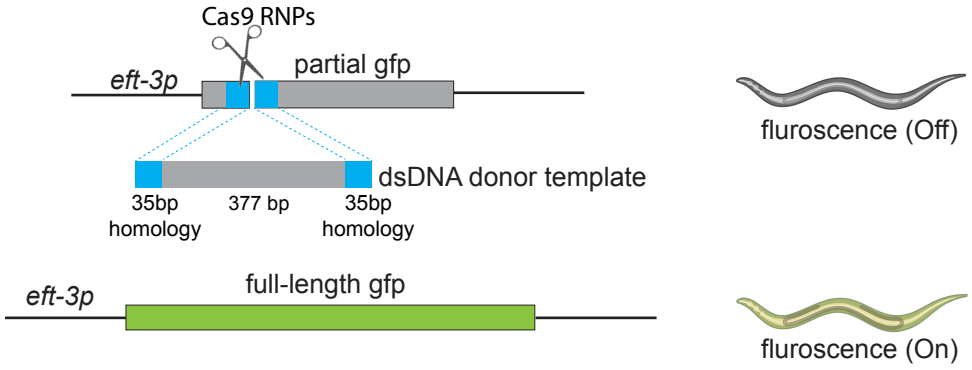

B

dsDNA donor type	GFP(+) F1s cloned	F2 transmission (%)
unmodified	40	40 (100)
TEG	39	39 (100)
2′OMe-RNA-TEG	36	36 (100)

Figure S5. Precise insertions are germline transmitted in *C. elegans*. (A) Schematic representaiton of the eft3p-gfp (partial) locus edited with dsDNA donors with or without end-modifucationS in *C. elegans*. Precisely edited animals express GFP signal ubiqutiously. (B) GFP-postive F1 animals were cloned and their progeny (F2s) were scored for GFP expression. Number of F1s that produced GFP expressing F2 in a mendelian fashion are shown under F2 transmission column.

Figure S6

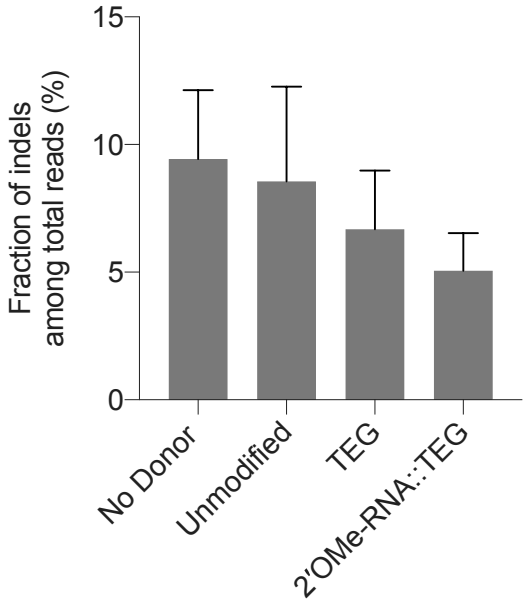

Figure S6 : Indel efficincies in zebrafish zygotes. (A) Fraction of reads with indels among total reads obtained in experiments with either no donor, unmodified or end-modified donors are plotted as percentage. Precise repair (HDR) efficiencies are shown in Figure 5A.

Figure S7

A

Microinjection information for targetted editing of the *Tyr* locus in Swiss-webster mice

Donor type	Zygotes transferred	Pups born	Pups with dark eyes (P2)	Pups alive (P10)	Pups with coat pigment (P10)	Coat color (% among P10 animals)		
						Uniform-HDR (Black/Agouti)	Mosaic HDR	Non-HDR (Albino)
Unmodified	169	56	7 (12.5%)	46	8 (17.4%)	5 (10.9%)	3 (6.5%)	38 (82.6%)
2′OMe-RNA-TEG	198	68	24 (35.3%)	66	25 (37.9%)	23 (34.9%)	2 (3.0%)	41 (62.1%)

Only pups that were alive on P10 were inlcuded in the analysis. Among the pups that died before P10 one pup (2′OMe-RNA-TEG group) exhibited dark eye phenotype.

B

Germline transmission of *Tyr*$^{c\text{-}cor}$ allele to F1 generation

Donor Type	F0 Mouse ID# (gender)	Number of F1 pups	number of F1 pups with TYR$^{C\text{-}Cor}$ (%)
Unmodified	1 (female)	11	5 (45.5)
	16 (male)	7	2 (28.5)
	20 (female)	14	8 (57.1)
	51 (male)	14	10 (71.4)
	54 (female)	15	8 (53.3)
	55 (female)	15	8 (53.3)
	59 (male)	17	6 (35.3)
	60 (male)	9	8 (88.9)
2′OMe-RNA-TEG	1 (male)	11	7 (63.6)
	6 (male)	12	6 (50)
	18 (female)	14	5 (35.7)
	22 (female)	14	6 (42.3)
	23 (female)	14	5 (35.7)
	24 (female)	13	9 (69.2)
	41 (male)	8	4 (50)
	42 (male)	9	4 (44.4)

C

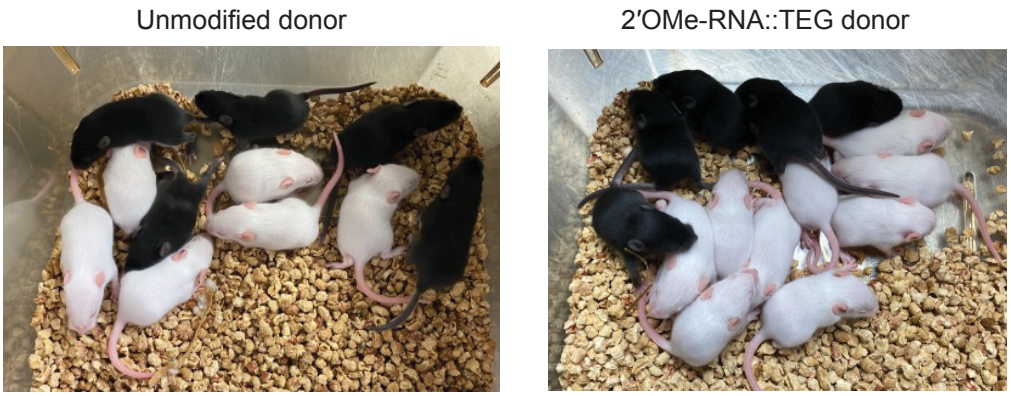

Figure S7. 5′ modified donors improve targetted editing efficiency at the *Tyr* locus in Albino mice. (A) Micro-injection information and HDR efficiencies obtained for unmodified and 2′OMe-RNA::TEG modified donors. (B) Germline transmission of the edited *Tyr*$^{c\text{-}cor}$ allele was confirmed by crossing some of the pigmented F0 mice to Swiss webster mice (*Tyr*^{c}) and phenotyping their F1 progeny (C) Representative images of F1 litters obtained from crosses for germline transmission tests.

Figure S8

A

Microinjection information for *V5* tag insertion at the *Sox2* locus

Donor type	Zygotes transferred	Pups born	Pups analyzed	HDR (% among analyzed)
Unmodified	214	36	35	2 (5.7%)
2′OMe-RNA-TEG	209	27	24	8 (33.3%)

1 pup from the unmodified donor group and 3 pups from 2′OMe-RNA-TEG donor group died at P3 and were not included in the analysis).

B

Germline transmission of *Sox2::V5* to F1 generation

Donor Type	F0 Mouse ID# (gender)	number of F1 pups	number of F1 pups with *Sox2::V5* (%)
Unmodified	6 (male)	18	14 (77.8)
2′OMe-RNA-TEG	10 (male)	10	5 (50)
	11 (male)	10	3 (30)
	12 (female)	6	4 (66.7)
	16 (female)	1	1 (100)
	17 (female)	5	3 (60)
	26 (male)	6	4 (66.7)

C

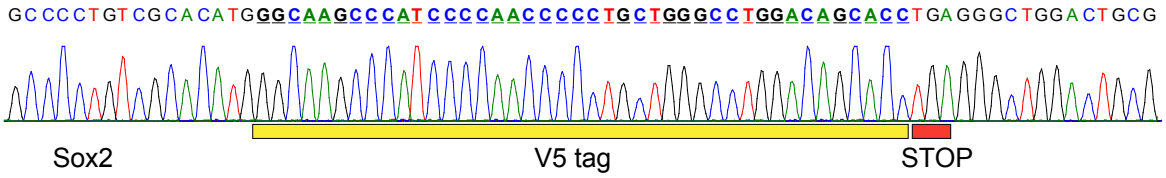

Figure S8. 5′ modified donors imporve targetted editing efficiency at the *Sox2* locus in mouse zygotes. (A) Microinjection information and HDR efficiencies obtained using unmodified and 2′OMe-RNA::TEG modified donors are shown. (B) Germline transmission rates of the *Sox2::V5* allele was confirmed by crossing the HDR positive F0 mice with WT mice and genotyping the F1 pups. (C). Sanger sequencing trace of *Sox2::V5* allele in F1 mice.

Figure S9

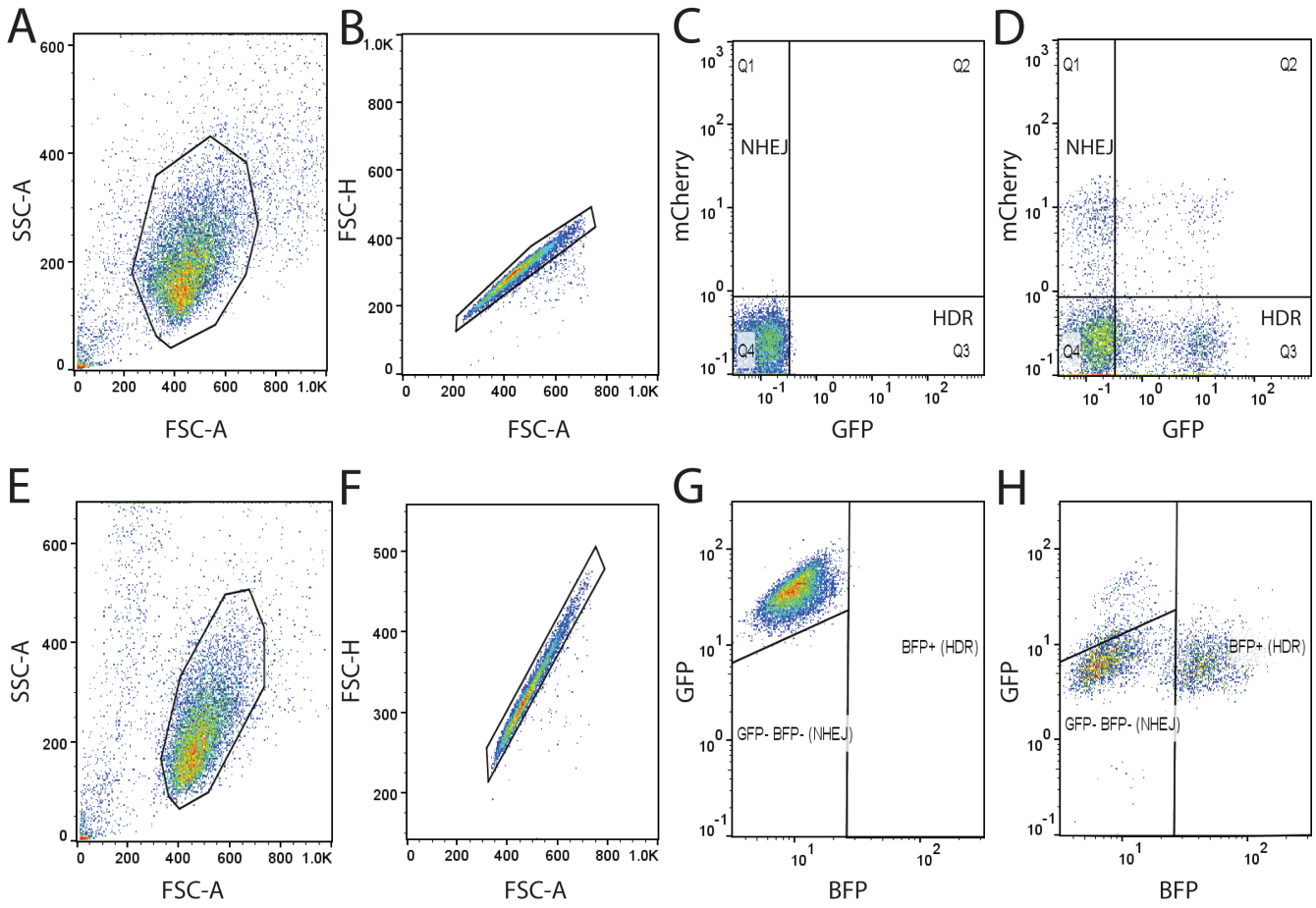

Figure S9. Flow cytometry analysis to determine the percentage of precise and imprecise genome editing events. The gating strategies used for HEK293T TLR cells (Top) and K562 GFP+ cells (Bottom) are shown. Cells were first gated based on forward and side scattering to select “live” cells (A, E), and then gated to select singlets (B, F). Quadrant gates were drawn to isolate GFP+ mCherry- cells (indicating successful HDR) and mCherry+ GFP- cells (indicating imprecise repair) for mock-transfected sample (C) and treated sample (D). G, H. K562 GFP+ cells were gated for BFP+ events (precise) and double-negative events (imprecise). Representative mock-transfected (G) and treated (H) samples are shown.

Materials and Methods

Synthesis of PNA-NLS peptide. PNA oligomers were synthesized at 2µmol scale on Fmoc-PAL-PEG-PS solid support (Applied Biosystems) using an Expedite 8909 synthesizer. Fmoc/Bhoc-protected PNA monomers (Link Technologies) were dissolved to 0.2M in anhydrous *N*-methylpyrrolidinone. Amino acid monomers (Sigma Aldrich) and AEEA linker (Link Technologies) were dissolved to 0.2 M in anhydrous dimethylformamide. Coupling time was 8.5 min using HATU (Alfa Aesar) as activator; double coupling was performed on all PNA monomers and amino acids. PNAs were cleaved and deprotected by treating the resin with 400 µL of 19:1 TFA:*m*-Cresol for 90 min at room temperature. The resin was then removed with a PTFE centrifugal filter and PNAs were precipitated from cold diethyl ether and resuspended in deionized water. PNAs were purified by HPLC on a Waters XSelect CSH C18 5µm column at 60 °C, using gradients of acetonitrile in water containing 0.1% TFA, and were characterized on an Agilent 6530 Q-TOF LC/MS system with electrospray ionization. The PNA::NLS sequence used was GCGCTCGGCCCTTCC-[AEEA linker]-PKKKRK.

Synthesis of PEGylated oligos. PEG-modified oligonucleotides were synthesized using standard phosphoramidite methods on an ABI 394 synthesizer. Phosphoramidites were purchased from ChemGenes. Coupling times for 2′OMe-RNA and spacer phosphoramidites were extended to 5 min. Oligonucleotides were deprotected in concentrated aqueous ammonia at 55 °C for 16 h. Oligonucleotides were desalted using either Nap-10 (Sephadex) columns or Amicon ultrafiltration. All the PEG-modified oligonucleotides were characterized on an Agilent 6530 Q-TOF LC/MS system with electrospray ionization. The 2′-OMe RNA sequence appended to the 5′-end of donor DNAs was GGAAGGGCCGAGCGC.

dsDNA Donor generation. Donor template sequences with the homology arms and the desired insert for knock-in (eg: gfp), were generated by PCR. PCR products were cloned into ZeroBlunt TOPO vector (Invitrogen, #450245) and plasmids were purified using Macherey-Nagel midi-prep kits (cat# 740412.50). Using the purified plasmids as templates and PEGylated oligos as primers, donor sequences were PCR amplified with Q5 (NEB, *C. elegans*) or Q5 or Phusion polymerase (NEB, mammalian). Before use in *C. elegans* microinjections, the resulting PEGylated PCR products were excised from 0.8-1% TAE agarose gel and purified using spin-columns (Omega, #D2501-02). For use in mammalian cells, the PEGylated long PCR products were purified using spin columns (Qiagen, # 28104) and short PCR products were gel-extracted (Omega, #D2501-02) and then purified again with Ampure XP beads.

Single Strand DNA donor generation. Long single stranded DNA donors were prepared using the protocol described by Li et al [1]. Briefly, the donor template containing the T7 promoter was amplified using standard PCR and purified using SPRI magnetic beads (Core Genomics). T7 *in vitro* transcription was performed using the HiScribe T7 High Yield RNA Synthesis kit (NEB) and the RNA was purified using the SPRI magnetic beads. Finally, the ssDNA donor was synthesized by TGIRT™-III (InGex) based reverse transcription using the synthesized RNA as a template and a TEG-modified or unmodified DNA primer. We then performed base-treatment to remove RNA. The donor was again purified using SPRI beads.

Expression and purification of SpyCas9. The pMCSG7 vector containing the 6xHis-tagged 3xNLS SpyCas9 was a gift from Scot Wolfe at UMass Medical School. This construct was transformed into the Rosetta 2 DE3 strain of *E. coli* for protein production. Expression and purification of SpyCas9 was performed as described previously [2]. Briefly, cells were grown at 37°C to OD600 of 0.6, at which point 1 mM IPTG (Sigma) was added and the temperature was

lowered to 18°C. Cells were grown overnight and harvested by centrifugation at 4,000 g. The protein was purified first by Ni^{2+} affinity chromatography, then by cation exchange and finally by size-exclusion chromatography.

Illumina sequencing (Mammalian cells)

Regions of interest were amplified from genomic DNA and sequenced on an Illumina MiniSeq platform. PCR1 ((98° C- 2min, 24 cycles of (98° C- 15sec, 64° C- 20sec, 72° C- 15sec), 72° C- 5min) was performed using 200ng gDNA, 1.25uL of 10uM forward and reverse primers that contain Illumina adapter sequences, 12.5uL NEBNext UltraII Q5 Master Mix, and water to bring the total volume to 25uL. PCR2 (98° C- 2min, 10 cycles of (98° C- 15sec, 64° C- 20sec, 72° C- 15sec), 72° C- 5min) was done using 1uL of unpurified PCR1 reaction mixture, 1.25 uL of 10uM forward and reverse primers that contain unique barcode sequences, 12.5uL NEBNext UltraII Q5 Master Mix, and water to bring the total volume to 25uL. PCR2 products were first analyzed using 2% agarose gel electrophoresis, and then similar amounts were pooled based on the band intensities. Pooled PCR2 products were first purified by gel extraction (Qiagen) and purified again by PCR cleanup columns (Qiagen). Concentration of final purified library was determined by Qubit (High Sensitivity DNA assay). The integrity of library was confirmed by Agilent Tapestation using Agilent High Sensitivity D1000 ScreenTape kit. The library was then sequenced on an Illumina Miniseq platform according to the manufacturer's instructions using MiniSeq Mid Output Kit (300-cycles). Sequencing reads were demultiplexed using bcl2fastq2 (Illumina) and CRISPResso2 [3] was used to align the reads and quantify editing efficiencies. Quantification window size was set as 30 to ensure the stringent analysis. HDR efficiency was calculated as percentage of (precise HDR reads) / (total reads).

Guide-Seq Experiment. Two phosphorothioate linkages were incorporated between the first three and the last three nucleotides in the dsODN tags. Unmodified dsODN does not contain any further modifications whereas modified dsODN contains 5′ TEG (SP9) modification (Integrated DNA Technologies). Sequencing libraries were prepared as previously described [4]. Data was processed and analyzed using the GUIDE-seq analysis software [4].

Cell culture and transfections. HEK293T cells were obtained from ATCC and were cultured in standard DMEM medium (Gibco, #11995) supplemented with 10% fetal bovine serum (FBS) (Sigma, #F0392). Human foreskin fibroblasts (HFF) were maintained in DMEM medium supplemented with 20% FBS. Chinese hamster ovary (CHO) cells (obtained from ATCC) were cultured in F-12K medium (Gibco 21127022) supplemented with 10% FBS, and K562 cells were cultured in IMDM medium (Gibco 12440053) supplemented with 10% FBS. Traffic Light Reporter Multi-Cas Variant 1 (TLR-MCV1) reporter cells were previously described [5]. Electroporations were performed using the Neon transfection system (ThermoFisher). SpyCas9 was delivered either as a plasmid or as protein. For plasmid delivery of Cas9 and sgRNA, appropriate amounts of plasmids were mixed in ~10 µl Neon buffer-R (ThermoFisher) followed by the addition of 100,000 cells. For RNP delivery of Cas9 (IDT), GFP-to-BFP assay (20 pmolCas9 and 25 pmol of crRNA-tracrRNA), EMX1-HEK293T (5pmol Cas9, 10pmol sgRNA (IDT)), EMX1-K562 (10pmol Cas9, 20pmol sgRNA), were mixed in 10 µl of buffer R. This mixture was incubated at room temperature for 30 minutes followed by the addition of 100,000 cells that were already resuspended in buffer R. This mixture was then electroporated using the 10 µl Neon tips. Electroporation parameters (pulse voltage, pulse width, number of pulses) were 1150 v, 20 ms, 2 pulses for HEK293T cells, 1650 v, 10 ms, 3 pulses for CHO cells, 1400 v, 30 ms, 1

pulse for HFF cells and 1600 v, 10 ms, 3 pulses for K562 cells. Electroporated cells were harvested for FACS analysis 48-72 hr post electroporation unless mentioned otherwise.

K562 GFP+ stable cell line generation. Lentiviral vector expressing EGFP was cloned using the Addgene plasmid #31482. The EGFP sequence was cloned downstream of the SFFV promoter using Gibson assembly. For lentivirus production, the lentiviral vector was co-transfected into HEK293T cells along with the packaging plasmids (Addgene 12260 & 12259) in 6-well plates using TransIT-LT1 transfection reagent (Mirus Bio) as recommended by the manufacturer. After 24 hours, the medium was aspirated from the transfected cells and replaced with fresh 1 ml of fresh DMEM media. The next day, the supernatant containing the virus from the transfected cells was collected and filtered through a 0.45 µm filter. 10 µl of the undiluted supernatant along with 2.5 µg of Polybrene was used to transduce ~1 million K562 cells in 6-well plates. The transduced cells were selected using media containing 2.5 µg/ml of puromycin. Less than 20% of the transduced cells survived, and these were then diluted into 96-well plates to select single clones. One of the K562 GFP+ clones was used for the analysis shown in this study. Cas9 was electroporated into the K562 GFP+ cells as RNP (20 pmol) with a crRNA targeting the *GFP* sequence. ssODN (66 nt) with or without end modifications was provided as donor template to convert the *GFP* coding sequence to the *BFP* coding sequence. % BFP (+) (HDR) and % GFP (-) BFP (-) (NHEJ) cells were quantified using flow cytometry.

Flow cytometry. The electroporated cells were analyzed on a MACSQuant VYB from Miltenyi Biotec. Cells were gated first based on forward and side scattering to select “live” cells and then for single cells. GFP-positive cells were identified using the blue laser (488 nm) and 525/50 nm

filter whereas for the detection of mCherry positive cells, yellow laser (561 nm) and 615/20 nm filter were used. BFP-positive cells were identified using the violet laser (405 nm) and 450±50 nm filter. The gating strategy is shown in **Figure S9**.

Southern Blotting to visualize donor concatemers.

dsDNA donors (566bp) were prepared using DIG labeled dUTP nucleotide mix ((Sigma Aldrich # 11585550910). 1.5 pmol of gel-extracted DNA was nucleofected into HEK293T (100,000) cells (Cas9 or guideRNAs were not added to the mix). Nucleofected cells were collected at various time points and pellets were frozen at -80° C until processed for DNA extraction. Total DNA was extracted using buffered Phenol: Chloroform: Isoamyl Alcohol and quantified using Qubit (HS-DNA). Total DNA (genomic + exogenous) of 200ng (0 hr to 24 hr) or about 800ng (48 hr and 72 hr) was used for agarose gel (0.8%) electrophoresis. Higher amounts of DNA were loaded for the later time points to blot for roughly equal amounts of exogenous DNA and to account for the increase in total cell number over the time course. 200pg of 566bp and 800pg of 13kb DIG labelled PCR DNA were used as size markers. After electrophoresis agarose gel was treated with 0.25N HCl (depurination) for 10 min followed by three washes with distilled water. The gel was then treated with denaturing solution (0.5M NaOH and 1.5M NaCl) for 20 min and another 30 min with fresh solution; followed by neutralization (2 washes 10 minutes each) with Alkaline transfer buffer (5xSSC with 10mM NaOH). Using Alkaline transfer buffer, DNA was then transferred for 3 hours with upward capillary action onto positively charged nylon membrane (Amersham Hybond N+, RPN303B). After transfer, membrane was soaked in 5xSSC for 10 min and UV crosslinked. Blots were then processed using DIG Wash and Block buffer set (Sigma Aldrich # 11585762001) according to the manufacturer's protocol. Briefly, membrane was blocked in 1x blocking solution

with Maleic acid for 30 min, incubated with 1:20,000 Anti-Digoxigenin-AP, Fab fragments (Sigma Aldrich # 11093274910) in 1x blocking solution for 1 hour, washed twice with 1x wash buffer, incubated in 1x detection buffer and developed using CDP-star (Sigma Aldrich # 12041677001).

***C. elegans* microinjection and HDR screening.** Microinjections were performed using Cas9-RNPs as previously described [6]. dsDNA donors were generated by PCR; 25ng/µl of unmodified or end-modified dsDNA donors were used in each injection mixture. Donors were heated and quick-cooled as previously described [6]. Starting strain that is homozygous for 3XFLAG::GlyGlyGly::TEV::CSR-1 allele was used to knock-in *gfp* sequence between flag and glycine-linker. crRNA (CTATAAAGACGATGACGATA NGG) with PAM site in the glycine-linker and donor DNA with arms homologous to 35 bp of 3xflag and 30 bp of 3xglycine-linker::tev flanking the gfp sequence were used. Loss of function WM702 (*eft3p::gfp(ne4807))* reporter strain was generated in EG6070 (oxSi221 [eft-3p::GFP + Cbr-unc-119(+)] II) strain background using CMG-48 and CMG-49 guides (See Supplemental Table S1). *Rol-6 (su1006)* plasmid was used as co-injection marker. This marker plasmid forms episomal non-integrating extrachromosomal elements that transiently mark a subset of progeny by causing them to exhibit an easily scored Roller phenotype. Under the conditions used, high quality injections into both gonad arms yielded 20 to 40 Roller progenies from each injected animal. For each donor type entire F1 broods from four or more injected animals were scored and tabulated the total number of GFP positive progeny and the number of GFP positive Roller progeny.

Zebrafish Experiments

Fish Care

Fish were maintained in accordance with the protocols set by the University of Massachusetts Medical School Institutional Animal Care and Use Committee. All the injections were performed into embryos derived from in-crosses of the EK wildtype line.

Zebrafish zygote microinjections

One cell-staged embryos were injected with 30pg of either unmodified or end-modified donors together with 24fmol RNP of modified Cas12a protein (Lb-2C-Cas12a) and modified crRNA (dr crRNA) per embryo as described previously [7], targeting 5′ end of the *hey2* coding sequence. Embryos were incubated for 24 hours post injection, genomic DNA was extracted and libraries for amplicon sequencing were prepared. For library construction, linear amplification using a single primer containing UMI was performed first, followed by PCRs for exponential amplification and barcode stitching were performed as described previously [7]. Quantification of the reads containing indels and precise knock-ins of Avi-tag was performed using the Python script deposited at the Github repository: (https://github.com/locusliu/PCR_Amplicon_target_deep_seq/blob/master/CRESA-lpp.py). All the experiments were performed in three independent replicates except injections with unmodified donors which were performed in duplicates.

Mouse Experiments

Strains and microinjection: All the mouse experiments were conducted according the UMMS Institute Animal Care and Use Committee (IACUC). C57BL/6J (Stock #000664) and Swiss Webster (Stock #SW) were obtained from Jackson Laboratory and Taconic respectively. All the

184 animals were maintained in a 12 hr light/dark cycle. Superovulated females were mated, and their
185 zygotes were collected at E0.5. Male pronuclei were injected with the injection mixtures described
186 below. Finally, zygotes were transferred to pseudo pregnant recipients and allowed to go to term.
187 Donor preparation: Using plasmids as templates and either unmodified or end-modified oligos as
188 primers, donor sequences were PCR amplified with Q5 polymerase (NEB). The resulting PCR
189 products were excised from 0.8% TAE agarose gel and purified using spin-columns (Omega,
190 #D2500). Gel-extracted DNA was further purified with 1.5X AMPure XP (Beckman Coulter)
191 beads according to the manufacture's protocol and eluted in nuclease free water. Before use in
192 microinjection mixes, dsDNA donors were subjected to heating and cooling protocol in thermal
193 cycler as described previously [6].
194 Injection Mixture preparation: Injections mixes were prepared with the following final
195 concentrations: S.p. Cas9 Protein (50 ng/µl) (IDT); S.p. Cas9 mRNA (50 ng/µl) (TriLink; L-7206);
196 sgRNA (20 ng/µl) (IDT); dsDNA donor (1 ng/µl). Cas9 protein, sgRNA and TE (pH 7.5) were
197 incubated at 37° C for 20 min. This mixture was then equally split into two tubes and the following
198 components were added to each tube: Cas9 mRNA, dsDNA donor (either unmodified or 5′ 2′OMe-
199 RNA::TEG modified), TE (pH 7.5) to bring the total volume to 50 µl. After pipetting well, the
200 final injection mixtures were centrifuged at 14,000g for 2 min and 46 µl was taken from the top
201 (to avoid particles that may clog the needles) and transferred to fresh tubes. All the steps were
202 performed at room temperature. Mixtures were kept on ice and directly loaded into the needles for
203 microinjection.
204 Genotyping: Tail clips of *Sox2-V5* founder animals were collected at P10, genotyped by PCR and
205 Sanger sequenced to confirm precise insertion. To confirm germline transmission, some of the

HDR positive F0 animals were mated with WT animals and tail clips of F1 animals were genotyped.

Oligo Sequences. Sequences of all the guide RNAs used in this study are provided in Supplemental Table S1 and sequences of all the oligos used are provided in Supplemental Table S2.

Statistics. All the statistical analyses were performed using GraphPad Prism. The type of analysis performed, and the P-value information can be found in respective figure legends.

Data availability. All the data supporting the findings of this study are available within the paper and supplementary information. Any other data related to this manuscript are available upon reasonable request.

References

1 Li, H. *et al.* Design and specificity of long ssDNA donors for CRISPR-based knock-in. *bioRxiv*, 178905, doi:10.1101/178905 (2019).

2 Jinek, M. *et al.* A programmable dual-RNA-guided DNA endonuclease in adaptive bacterial immunity. *Science* **337**, 816-821, doi:10.1126/science.1225829 (2012).

3 Clement, K. *et al.* CRISPResso2 provides accurate and rapid genome editing sequence analysis. *Nat Biotechnol* **37**, 224-226, doi:10.1038/s41587-019-0032-3 (2019).

4 Tsai, S. Q. *et al.* GUIDE-seq enables genome-wide profiling of off-target cleavage by CRISPR-Cas nucleases. *Nat Biotechnol* **33**, 187-197, doi:10.1038/nbt.3117 (2015).

5 Iyer, S. *et al.* Efficient Homology-directed Repair with Circular ssDNA Donors. *bioRxiv*, 864199, doi:10.1101/864199 (2019).

6 Ghanta, K. S. & Mello, C. C. Melting dsDNA Donor Molecules Greatly Improves Precision Genome Editing in Caenorhabditis elegans. *Genetics* **216**, 643-650, doi:10.1534/genetics.120.303564 (2020).

7 Liu, P. *et al.* Enhanced Cas12a editing in mammalian cells and zebrafish. *Nucleic Acids Res* **47**, 4169-4180, doi:10.1093/nar/gkz184 (2019).